การออกแบบและพัฒนากระบวนการผลิตเอทิลีนคาร์บอเนตจากชีวมวล

นายหัฏฐะชัย เอี้ยวเจริญลาภ

วิทยานิพนธ์นี้เป็นส่วนหนึ่งของการศึกษาตามหลักสูตรปริญญาวิศวกรรมศาสตรมหาบัณฑิต
สาขาวิชาวิศวกรรมเคมี ภาควิชาวิศวกรรมเคมี
คณะวิศวกรรมศาสตร์ จุฬาลงกรณ์มหาวิทยาลัย
ปีการศึกษา 2556

DESIGN AND DEVELOPMENT OF ETHYLENE CARBONATE PRODUCTION PROCESS FROM BIOMASS

Mr. Hattachai Aeowjaroenlap

A Thesis Submitted in Partial Fulfillment of the Requirements

for the Degree of Master of Engineering Program in Chemical Engineering

Department of Chemical Engineering

Faculty of Engineering

Chulalongkorn University

Academic Year 2013

Thesis Title	DESIGN AND DEVELOPMENT OF ETHYLENE CARBONATE PRODUCTION PROCESS FROM BIOMASS
By	Mr. Hattachai Aeowjaroenlap
Field of Study	Chemical Engineering
Thesis Advisor	Professor Suttichai Assabumrungrat, Ph.D.
Thesis Co-Advisor	Wisitsree Wiyaratn, Ph.D.

Accepted by the Faculty of Engineering, Chulalongkorn University in Partial Fulfillment of the Requirements for the Master's Degree

.....Dean of the Faculty of Engineering

(Professor Bundit Eua-arporn, Ph.D.)

THESIS COMMITTEE

.....Chairman

(Assistant Professor Soorathep Kheawhom, Ph.D.)

.....Thesis Advisor

(Professor Suttichai Assabumrungrat, Ph.D.)

.....Thesis Co-Advisor

(Wisitsree Wiyaratn, Ph.D.)

.....Examiner

(Associate Professor Artiwan Shotipruk, Ph.D.)

.....External Examiner

(Associate Professor Navadol Laosiripojana, Ph.D.)

หัฏฐะชัย เอี้ยวเจริญลาภ : การออกแบบและพัฒนากระบวนการผลิตเอทิลีนคาร์บอเนตจากชีวมวล. (DESIGN AND DEVELOPMENT OF ETHYLENE CARBONATE PRODUCTION PROCESS FROM BIOMASS) อ.ที่ปรึกษาวิทยานิพนธ์หลัก: ศ. ดร. สุทธิชัย อัสสะบำรุงรัตน์, อ.ที่ปรึกษาวิทยานิพนธ์ร่วม: ดร.วิศิษฏ์ศรี วิยะรัตน์, , 95หน้า.

งานวิจัยนี้ได้ศึกษาการออกแบบและพัฒนากระบวนการผลิตเอทิลีนคาร์บอเนตจากชีวมวล กระบวนการทั้งหมดประกอบด้วย 4 ส่วนหลัก ได้แก่ กระบวนการผลิตก๊าซชีวภาพจากชีวมวล โดยใช้กระบวนการย่อยสลายแบบไม่ใช้ออกซิเจน, กระบวนการผลิตสารประกอบไฮโดรคาร์บอนที่มี 2 อะตอม โดยใช้ปฏิกิริยาการคู่ควบมีเทน, กระบวนการผลิตเอทิลีนออกไซด์ และกระบวนการผลิตเอทิลีนคาร์บอเนต ก๊าซชีวภาพที่ผลิตได้ จะผ่านกระบวนการกำจัดคาร์บอนไดออกไซด์ ก่อนจะนำไปผลิตสารประกอบไฮโดรคาร์บอน 2 อะตอม โดยใช้ปฏิกิริยาการคู่ควบมีเทน บนตัวเร่งปฏิกิริยา Na-W-Mn/SiO2 เอทิลีนที่เกิดขึ้นจะถูกนำไปผลิตเอทิลีนออกไซด์และเอทิลีนคาร์บอเนตตามลำดับ โดยมีการใช้คาร์บอนไดออกไซด์ที่เกิดขึ้นจากส่วนอื่นของกระบวนการมาเป็นสารตั้งต้นในการผลิต กระบวนการผลิตถูกจำลองขึ้นด้วยโปรแกรม Aspen Plus® โดยมีการใช้สมการอธิบายจลน์ศาสตร์การเกิดปฏิกิริยา สำหรับปฏิกิริยาคู่ควบมีเทน และปฏิกิริยาการผลิตเอทิลีนออกไซด์ ที่มีการรายงานไว้ในงานวิจัยที่ผ่านมา งานวิจัยนี้ได้ศึกษาผลของตัวแปรหลักที่มีต่อประสิทธิภาพการผลิต ได้แก่ ปริมาณออกซิเจนที่ป้อนเข้าสู่กระบวนการคู่ควบมีเทน อุณหภูมิในการเกิดปฏิกิริยาคู่ควบมีเทน ปริมาณออกซิเจนที่ป้อนเข้าสู่กระบวนการผลิตเอทิลีนออกไซด์ และอุณหภูมิในการเกิดปฏิกิริยาการผลิตเอทิลีนออกไซด์ กระบวนการผลิตที่ปรับปรุงแล้ว ให้ค่าการเปลี่ยนมีเทนเท่ากับ 99.98% และให้ค่าร้อยละผลได้ของเอทิลีนเท่ากับ 27.47% ซึ่งเอทิลีนจะถูกนำไปผลิตเป็นเอทิลีนออกไซด์และเอทิลีนคาร์บอเนตตามลำดับ โดยมีการใช้คาร์บอนไดออกไซด์ที่เกิดขึ้นภายในกระบวนการไปเท่ากับ 27.54% กระบวนการผลิตที่ปรับปรุงแล้ว จะนำไปทำการบูรณาการเชิงพลังงาน โดยกระบวนการที่ผ่านการบูรณาการแล้วจะใช้พลังงาน 465 กิโลวัตต์ต่อกิโลโมลต่อชั่วโมงของเอทิลีน ซึ่งลดลงจากกระบวนการในกรณีตั้งต้นประมาณ 70% กระบวนการผลิตเอทิลีนคาร์บอเนตจากชีวมวลนี้ เป็นการนำเทคโนโลยีสะอาดที่ใช้สารชีวมวลมาเป็นสารตั้งต้นในการผลิต รวมถึงมีการใช้คาร์บอนไดออกไซด์ที่เกิดขึ้นภายในกระบวนการให้เป็นประโยชน์

ภาควิชา วิศวกรรมเคมี ลายมือชื่อนิสิต .....

สาขาวิชา วิศวกรรมเคมี ลายมือชื่อ อ.ที่ปรึกษาวิทยานิพนธ์หลัก .....

ปีการศึกษา 2556 ลายมือชื่อ อ.ที่ปรึกษาวิทยานิพนธ์ร่วม .....

5570440821 : MAJOR CHEMICAL ENGINEERING
KEYWORDS: OXIDATIVE COUPLING OF METHANE (OCM) / BIOMASS / ETHYLENE OXIDE / ETHYLENE CARBONATE / PROCESS SIMULATION / ASPEN PLUS

HATTACHAI AEOWJAROENLAP: DESIGN AND DEVELOPMENT OF ETHYLENE CARBONATE PRODUCTION PROCESS FROM BIOMASS. ADVISOR: PROF. SUTTICHAI ASSABUMRUNGRAT, Ph.D., CO-ADVISOR: WISITSREE WIYARATN, Ph.D., 95pp.

This research studied the design and development of ethylene carbonate production process from biomass. The overall process consisted of four sections including biogas production and treatment; oxidative coupling of methane (OCM) process; ethylene oxide (EO) process and ethylene carbonate (EC) process. Biogas was produced by a novel anaerobic digestion process and then treated to remove carbon dioxide. OCM reaction on Na-W-Mn/SiO2 catalyst was employed to produce ethane and ethylene (C2) products. Ethylene was then converted to ethylene oxide and ethylene carbonate by utilizing carbon dioxide generated from other parts of the process. Process simulation was performed by Aspen Plus® program. Novel kinetic model of OCM and EO had been employed in the developed process. Four key parameters of the process i.e. oxygen feed flow rate for OCM process, OCM reaction temperature, oxygen feed flow rate for EO process and EO reaction temperature were studied. The optimized process converts 99.98% of methane in biogas and yields 27.47% of ethylene, which consecutively converts into ethylene carbonate by utilizing 27.54% of carbon dioxide generated from the process. Process heat integration was performed in the optimized model. The heat-integrated process required 465 kW of energy consumption, which is about 70% reduction from the base case model. This process provides a green chemical concept, which uses biomass as raw materials and utilizes carbon dioxide generated to produce a higher valuable chemical.

Department:	Chemical Engineering	Student's Signature .....
Field of Study:	Chemical Engineering	Advisor's Signature .....
Academic Year:	2013	Co-Advisor's Signature .....

ACKNOWLEDGEMENTS

The author would like to express his highest thankfulness to Professor Dr.Suttichai Assabumrungrat, advisor and Dr.Wisitsree Wiyaratn, co-advisor for their inspiration, motivation, assistance and support throughout this research study. Moreover, the authors wish to thank Assistant Professor Dr.Suratep Kheawhom, as the chairman, Associate Professor Dr.Artiwan Shotipruk and Associate Professor Dr.Navadol Laosiripojana as the members of the thesis committee for their useful comments.

Most of all, the author would like to express his highest gratitude to his beloved parents, brother and sister.

Finally, grateful thanks to all members of Center of Excellence on Catalysis and Catalytic Reaction Engineering and Center of Excellence in Particle Technology, Department of Chemical Engineering, Chulalongkorn University.

CONTENTS

Page

Page

Page

LIST OF FIGURES

LIST OF TABLES

CHAPTER I

INTRODUCTION

1.1 Introduction

Carbon dioxide is known as a significant greenhouse gas, which is the cause of environmental effect nowadays. Carbon dioxide has no effect with the incoming short-wave radiation sun ray, but it absorbs the long-wave radiation reflected from the ground. This phenomenon, which results in increasing of the world temperature, called the greenhouse effect (Shimekit et al., 2012). The level of carbon dioxide in atmosphere increases corresponding with the number of chemical plant, somewhat generated from chemical reaction. Carbon dioxide release rate from chemical plant to atmosphere can be decreased by many ways. As one of the by-product from many oxidation reactions, carbon-dioxide is mainly used to synthesis other valuable chemicals such as urea (NH_2CONH_2), methanol (CH_3OH) from synthesis gas and also carbonate (CO_3^{2-}) compounds (Pierantozzi, 2001).

Ethylene carbonate ($C_2H_4CO_3$) synthesis is another way to utilize carbon dioxide from the reaction of ethylene oxide ($(C_2H_4)_2O$) and carbon dioxide. Ethylene oxide (Oxirane or Epoxy ethane) is obtained by direct oxidation of ethylene in the presence of silver based catalyst ($2C_2H_4 + O_2 \rightarrow (C_2H_4)_2O$; Lefort, 1931). However, the complete combustion of ethylene is likely to occur, resulted in generation of carbon dioxide ($C_2H_4 + 3O_2 \rightarrow CO_2 + H_2O$).

Recently, conventional route for ethylene production is the steam cracking process of higher hydrocarbons feedstock such as naphtha. Nevertheless, many researchers have dedicated to find alternative routes for the production of ethylene in order to reduce the consumption rate of naphtha. Methane is considered to be an alternative feedstock for ethylene production because it is a major component in natural gas. Ethylene synthesis from the Oxidative Coupling of Methane (OCM)

becomes an interesting route because it provides an alternative way to use methane as a petrochemical feedstock (Keller et al., 1982). Nonetheless, as reported from many researchers, there are several reactions occur simultaneously in the OCM reaction network and the complete combustion to form carbon dioxide is known as the major side reaction (Lee et al., 2012).

Biomass is widely known as the alternative-renewable source of hydrocarbon from nature. Use of biomass as raw material has more potential in chemical industry because of the ability to produce higher valuable products instead of using petrochemical feedstock. Use of biomass to produce biogas, which is mainly of methane (Shafei et al., 2013), by using the anaerobic digestion method is another way to utilize biomass effectively. Biogas produced is primarily methane and carbon dioxide which requires a treatment process to remove carbon dioxide in gas mixture before further use of methane. Thus, the biogas treatment process also results in releasing of carbon dioxide to atmosphere.

In this study, ethylene carbonate production process is considered as a carbon dioxide utilization method. Three main sources of carbon dioxide; from biogas treatment, generated as a by-product from oxidative coupling of methane and by-product from direct oxidation of ethylene to ethylene oxide, is utilized by reacting with ethylene oxide to form ethylene carbonate. The advantages of developed process are to reduce carbon dioxide released to the air by forming a green chemical concept that increase valuable of the product from the combination of oxidative coupling of methane and direct oxidation of ethylene process. This process also takes advantage of using biogas, which is a green-renewable resource, as a feedstock to produce higher valuable chemical instead of the conventional way that use raw materials from petroleum.

1.2 Objective

To develop a new ethylene carbonate production process from biomass, that utilize the carbon dioxide generated, by the reaction with the effluent from the combination process of oxidative coupling of methane and direct oxidation of ethylene.

1.3 Scope of work

1. Study the principle of each section in the overall process i.e.
   - Biogas production from biomass, which is wheat straw, at a production rate of 200,000 tons per year (dry weight) and principle of biogas treatment (CO_2 removing).
   - C2 production by the oxidative coupling of methane.
   - Ethylene oxide production by direct oxidation of ethylene.
   - Ethylene carbonate production by the reaction of ethylene oxide and carbon dioxide.
2. Develop the process flow diagram of each section in Aspen Plus, the conceptual diagram is shown in Figure 1.1

(a)

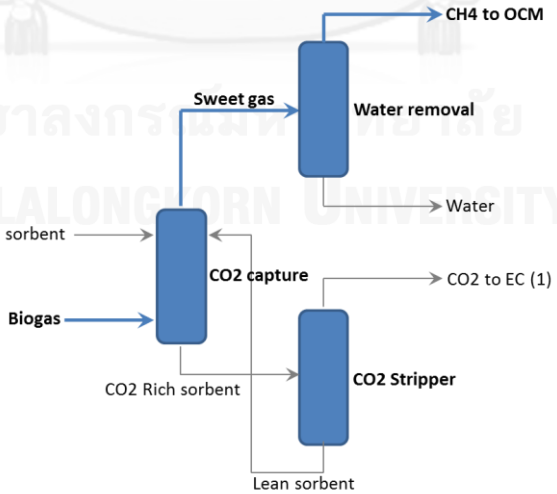

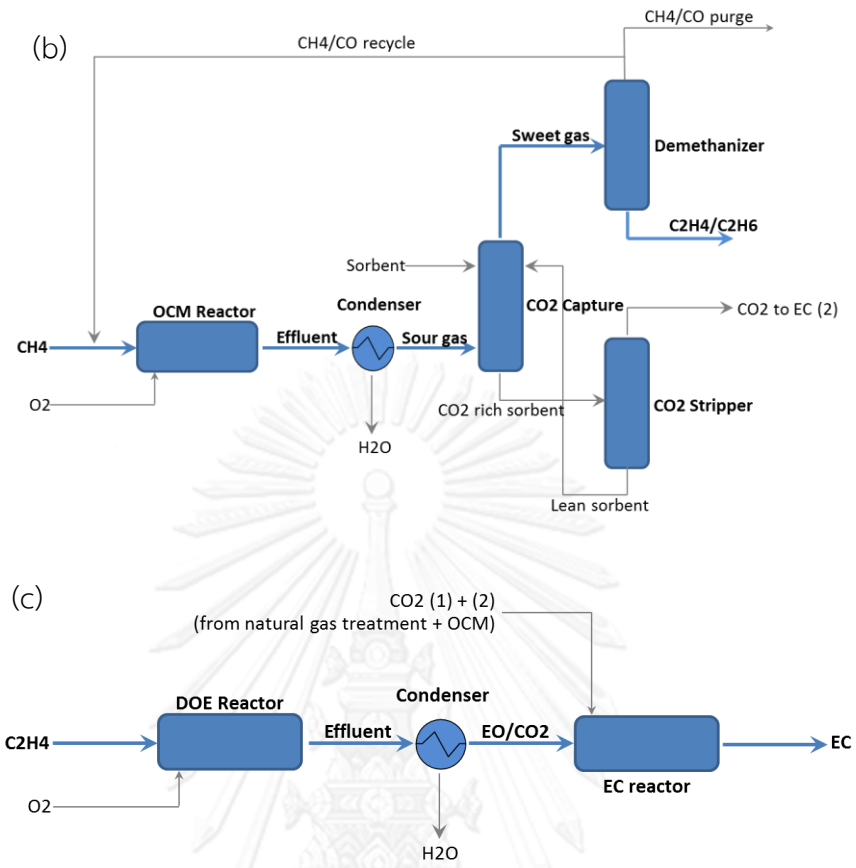

Figure 1.1 Conceptual designs for; (a) biogas treatment, (b) oxidative coupling of methane, (c) direct oxidation of ethylene and reaction of ethylene oxide to form ethylene carbonate

3. Develop the model for ethylene carbonate production process by utilizing the CO_2 generated from each section, the conceptual design of overall process is shown in Figure 1.2.

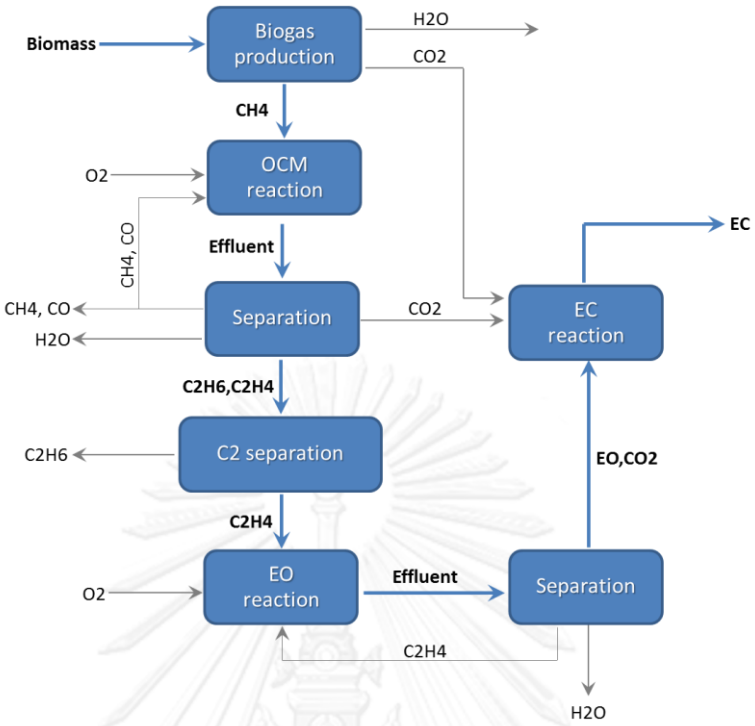

Figure 1.2 Conceptual design of overall process

4. Study the key parameters of the process i.e. oxygen feed flow rate, OCM reaction temperature and direct oxidation of ethylene reaction temperature on amount of CO2 emission, product yield and conversion of methane.
5. Perform process heat integration.

CHAPTER II

THEORIES

2.1 Biogas production

Biogas is used to call a gas mixture produced by organic compounds in absence of oxygen. Biogas can be obtained by anaerobic digestion with anaerobic bacteria or fermentation from bio-materials such as municipal wastes, manure, residual papers or plant crops. Main components in biogas are primarily methane and carbon dioxide with a small amount of siloxane, moisture and hydrogen sulfide. Biogas can be used to generate energy by the combustion with oxygen. This process allows the use of biogas as a renewable fuel. As known that methane is a primary component in biogas, it could be compressed to be a bio-CNG or use as a replacement of natural gas feedstock. (National Non-Food Crops Centre, 2011)

Anaerobic digestion, as mentioned before, is a technical method that digests biomaterials via an anaerobic microorganism in absence of oxygen. The process occurs in sequence of hydrolysis of raw materials, conversion by acidogenic bacteria called acidogenesis, further digestion by acetogen called acetogenesis and finally the formation of methane and carbon dioxide by methanogen called methanogenesis (WASTE, NL, 2007). Figure 2.1 shows the aforementioned anaerobic digestion process.

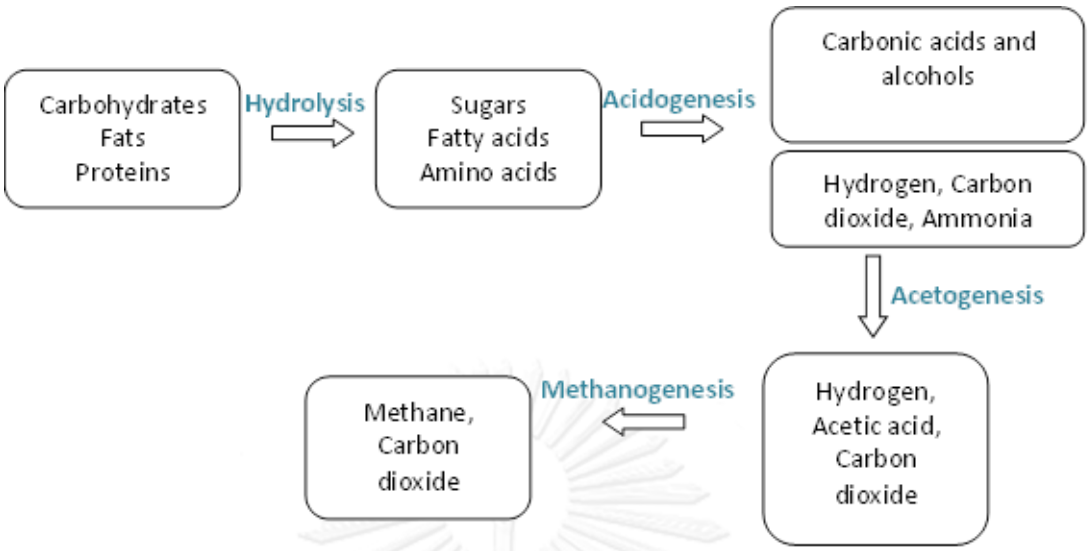

Figure 2.1 Schematic diagram of anaerobic digestion

As the biomass is a complex molecule that includes long chains of organic polymers, at first, it is broken down to be smaller molecules such as simple sugars, fatty acids or amino acids that available for anaerobic bacteria by the hydrolysis (Sleat, R. & Mah, R., 2006). Acidogenic bacteria then convert sugars, fatty acids and amino acids into carbonic acids along with alcohols, hydrogen, carbon dioxide and ammonia by the acidogenesis (Inria-Fr, 2007). Then the simple molecules created by acidogenesis are further digested by acetogenic bacteria resulting in acetic acid, carbon dioxide and hydrogen. Finally, methanogenic bacteria convert all intermediate molecules into methane and carbon dioxide and water. Table 2.1 shows the typical composition of biogas (Kolumbus, Fi, 2007)

Table 2.1 Typical biogas composition

Component	Composition (%)
Methane	50-75
Carbon dioxide	25-50
Nitrogen	0-10
Hydrogen sulfide	0-3
Oxygen	0-2

2.2 Carbon dioxide capture by amine absorption

Amines are derivative organic compounds of ammonia (NH_3). One or more hydrogen atoms have been substituted with an alkyl or aromatic group. The (–NH2) functional group of the amine molecule provides a weak base that can react with the acid gases. The absorption of CO2 occurs in a two-step reaction: (1) the dissolution of the gas in the aqueous solution and (2) there action of the weak acid gas with the weak basic amine. The first physical absorption step is determined by the partial pressure of the CO_2 in the gas feed. The reactions in the second step of CO2 absorption in aqueous amines have been widely studied, with a large number of reference materials on the reaction mechanisms (Bindwaletal., 2011; Kohl and Nielsen, 1997; Penny and Ritter, 1983; Vaidya and Kenig, 2007; Versteegetal., 1996) and guidelines for process operation (GPSA Engineering Data Book, 2004) available in the literature. The fundamental reactions involved in CO_2 absorption in amine treating are (Kohl and Nielsen, 1997):

Water dissociation:

$$H_2O \leftrightarrow H^+ + OH^- \tag{2.1}$$

CO2 dissolving and hydrolysis

$$CO_2 + H_2O \leftrightarrow HCO_3^- + H^+ \tag{2.2}$$

Protonation of the amine

$$RNH_2 + H^+ \leftrightarrow RNH_3 \tag{2.3}$$

Formation of the carbamate

$$RNH_2 + CO_2 \leftrightarrow RNHCOO^- + H^+ \tag{2.4}$$

Amines could be divided as primary (R-NH2), secondary (R-NH-R') and tertiary (R-NR'-R'') where R is a hydrocarbon chain. For primary and secondary amine, such as Monoethanolamine (MEA) and Diethanolamine (DEA), Overall reaction is predominated by the formation of carbamate (Eq. 2.4).Thus, the capacity or primary andsecondary amine is limited to about 0.5 mole of CO2 per mole of amine according to the stoichiometry of the reaction (Kidnay and Parrish, 2006).

However,tertiary amine such as MDEA (Methyldiethanolamine) do not have a free hydrogen atom bonded with nitrogen, therefore, tertiary amine do not react with CO2 directly to form the carbamate. In addition, reaction between CO2 and tertiary amine can be explained in equivalent of reaction (2.2) and (2.3), which are much slower than reaction (2.4) and the overall reaction is:

$$RR'R''N + CO_2 + H_2O \leftrightarrow RRR''NH^+ + HCO_3^- \quad (2.5)$$

The stoichiometry of reaction (2.5) shows that tertiary amine can load 1 mole of CO2 per mole of amine theoretically, which is more than the capacity of primary and secondary amine. Moreover, the heat of regeneration for tertiary amine is also lower. But, in contrast, the drawback of tertiary amine is the ability to absorb CO2, which is slower than primary and secondary amine. To solve that problem, an activator might be added in order to enhance the kinetic of CO2 absorption for tertiary amine by increasing the rate of hydrolysis of carbamate specie and dissolving of CO2 as well (GPSA Engineering Data Book, 2004)

2.3 Oxidative Coupling of Methane (OCM)

From a number of previous studies, the way to convert methane, which is the main component in natural gas, to be higher value chemicals has been received much attention from researchers. OCM is one of the interesting ways to convert methane to ethane and ethylene. Ethylene is known as a very basic raw materials used in petrochemicals industry; such as production of Polyethylene (PE), Polyethylene terephthalate (PET), Ethylene oxide (EO) etc.

2.3.1 Definition

Figure 2.2 shows the generalize mechanism of OCM reaction network. The reaction is start by the adsorption of oxygen molecules on the catalyst surface, and then follows by the activation of methane to form methyl radicals. Ethane is formed

by the coupling of methyl radicals and then is reacted with oxygen on the catalyst surface, resulted in formation of ethylene. The overall reaction is highly exothermic.

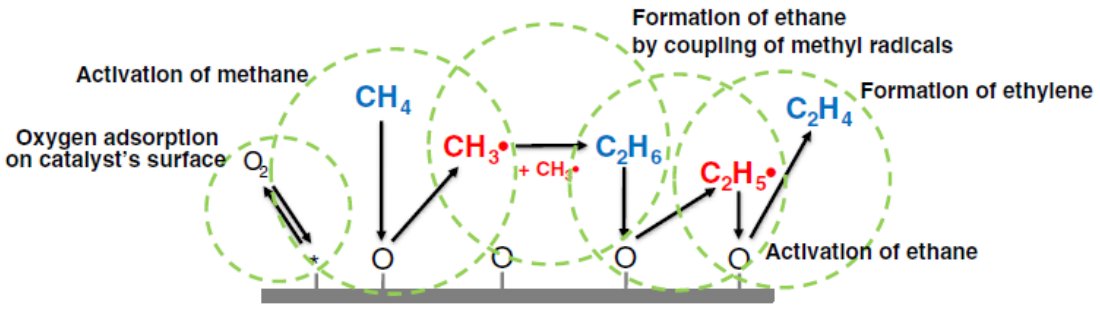

Figure 2.2 Reaction mechanism of the Oxidative Coupling of Methane (Lee *et al.*, 2012)

However, the selectivity of ethane and ethylene is mostly reduced by the formation of carbon monoxide and carbon dioxide from the combustion between oxygen and the effluents from reaction, which is likely to occur.

2.3.2 Mechanisms

About the mechanism of oxidative coupling of methane, it is widely known that methane is first reacted to form methyl radicals on the catalyst surface and then, methyl radicals are coupled into ethane in the gas phase. So, ethane is then dehydrogenated to ethylene. Nevertheless, in the presence of oxygen and hydrocarbons, the combustion is inevitably occurred and results in the formation of carbon monoxide and carbon dioxide which decrease the yield and selectivity of C_2 products.

The mechanisms are shown below (Gao*et al.*, 2010).

$$CH_4 + O^* \longrightarrow CH\bullet_3 + HO^* \quad (2.6)$$

$$HO^* + HO^* \longrightarrow H_2O + O^* \quad (2.7)$$

$$CH\bullet_3 + CH\bullet_3 \longrightarrow C_2H_6 \quad (2.8)$$

Overall reaction of the three steps above is shown below

$$2CH_4 + O^* \longrightarrow C_2H_6 + H_2O \quad (2.9)$$

Ethylene is secondly formed from oxydehydrogenation of ethane

$$C_2H_6 + 0.5O_2 \longrightarrow C_2H_4 + H_2O \quad (2.10)$$

$CH\bullet_3$ is methyl radical.

O* is surface active oxygen species.

2.4 Direct oxidation of ethylene

Ethylene oxide, also known as 'Oxirane', is the cyclic ether with the chemical formula C_2H_4O. According to the chemical structure of ethylene oxide, which is the simplest epoxide (shown in Figure 2.3), addition reaction can be occurred easily.

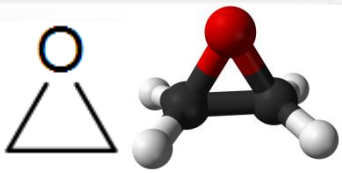

Figure 2.3 Chemical structure of ethylene oxide

(wikipedia.org/ethylene_oxide)

Ethylene oxide is the main reactant used in several chemical processes, i.e. for production of ethanolamine, ethylene glycol, simple and complex glycols as well as polyglycols, ethylene carbonate etc. In 1914, commercial production of ethylene oxide started from the BASF's chlorohydrin process. However, the chlorohydrin process obtained less attention because of low efficiencies and loss of chlorine reactant into calcium chloride (J.F. Norris *et a.l,* 1919). Ethylene oxide is industrially

produced by the direct oxidation of ethylene, which is firstly patented by Lefort (1931).

2.4.1 Definition

Ethylene oxide is commonly generated by the direct oxidation of ethylene at 230-280°C and 1-3 MPa on supported Ag catalyst. By the way, the complete combustion of ethylene and ethylene oxide can also occur at the same time. The direct oxidation of ethylene to ethylene oxide is mildly exothermic (ΔH = -105 kJ/mol) while the complete combustion of ethylene and ethylene oxide are extremely exothermic (ΔH = -1326 and -1222 kJ/mol). The reaction network is shown in Figure 2.4.

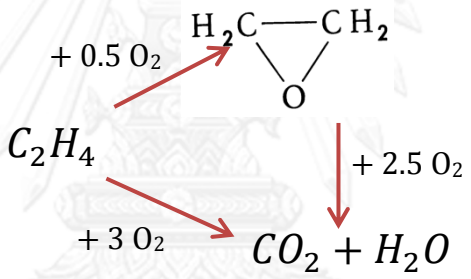

Figure 2.4 Reaction network of ethylene oxidation

Due to the extremely high heat of reaction and the undesired side reaction, the control of process condition and catalyst activity is definitely required. More in detail, the reaction conditions, e.g. temperature and pressure, affect the catalyst activity and reactant concentration in gas phase and, the catalyst design including acidity and surface concentration of the active site; affect the selectivity of ethylene oxide as well (van Santen *et al*, 1997). Furthermore, ethylene oxide can be oxidized consecutively to CO_2 and H_2O which decreases yield and selectivity of ethylene oxide. The mentioned side reaction is favored by high temperature and acidity of catalyst surface. Therefore, temperature control and surface acidity of catalyst are the major variables that need to be monitored closely.

2.4.2 Mechanisms

The heterogeneous catalytic oxidation of ethylene over Ag based catalyst was studied and proposed by P.A. Kilty and W.M.H. Sachtler in 1974. The mechanisms are as follow;

$$O_2 + 4\ Ag(adj) \longrightarrow 4\ Ag + 2\ O^{2-}(ads) \quad (2.11)$$

$$O_2 + Ag \longrightarrow Ag^{+} + O_2^{-} \quad (2.12)$$

$$O_2^{-}(ads) + CH_2{=}CH_2 \longrightarrow (CH_2CH_2)O + O(ads) \quad (2.13)$$

$$6\ O(ads) + CH_2{=}CH_2 \longrightarrow 2\ CO_2 + 2\ H_2O \quad (2.14)$$

Where (ads) refers to the molecule adsorbed on the catalyst surface and (adj) refers to oxygen atoms directly adjacent to silver particles. Thus, the following is the overall reaction;

$$7\ CH_2{=}CH_2 + 6\ O_2 \longrightarrow 6\ (CH_2CH_2)O + 2\ CO_2 + 2\ H_2O \quad (2.15)$$

The process temperature was optimized as 220–280 °C. Lower temperatures reduce the activity of the catalyst, and higher temperatures promote the complete oxidation of ethylene thereby reducing the yield of ethylene oxide. Elevated pressure of 1–3 MPa increases the productivity of the catalyst and facilitates absorption of ethylene oxide from the reacting gases.

Whereas oxidation by air is still being used, oxygen (> 95% purity) is preferred for several reasons, such as higher molar yield of ethylene oxide (75–82% for oxygen vs. 63–75% for air), higher reaction rate (no gas dilution) and no need of separating nitrogen in the reaction products.

2.5 Cycloaddition of carbon dioxide

By far, most of cyclic carbonates have been produced by the cycloadditon of carbon dioxide (or carbon dioxide cyclization). The reaction of oxiranes with carbon

dioxide leads to the generation of cyclic or polymeric carbonate, the mechanism is shown in Figure 2.5 (G.W.Coates et al., 2004).

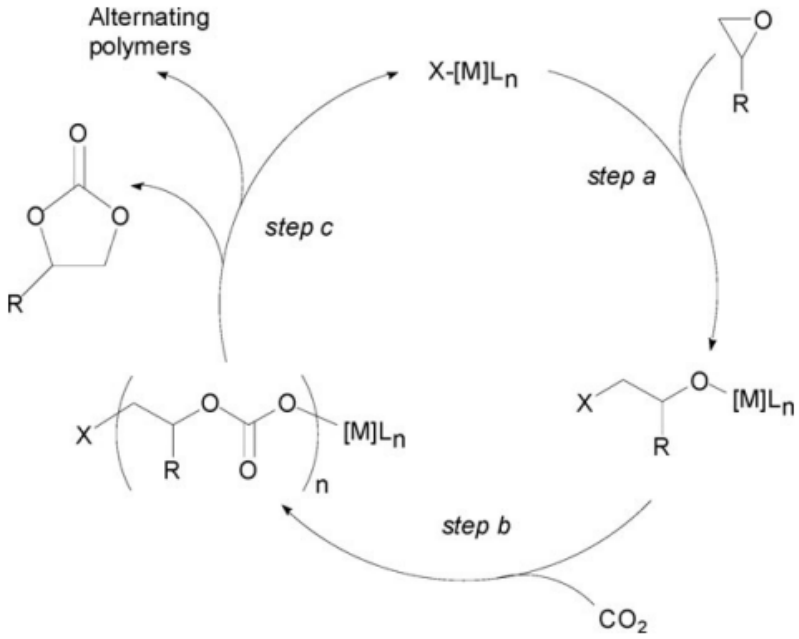

Figure 2.5 Cyclization of carbon dioxide to form a cyclic carbonate

Cyclic carbonates take an important role as an intermediate of the reaction pathway to form polycarbonates. Because most of polycarbonates nowadays is produced using the phosgene (T. Sakakura *et al.,* 2009) which is a highly toxic component, the cyclization of carbon dioxide is promising way of CO_2 utilization and phosgene substitution.

Ethylene carbonate is produced conventionally by reaction of ethylene oxide and carbon dioxide at 190-200 $^{\circ}C$ and 80 atm using Et4NBr catalyst (J.A. Riddick *et al.*, 1985) as in equation 2.16.

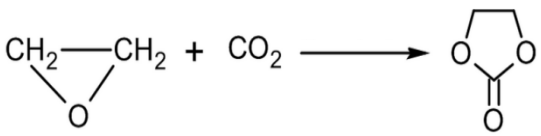

(2.16)

Ethylene carbonate is one of the four industrially important organic carbonates (Dimythyl carbonate, DMC; Diphenyl carbonate, DPC; Ethylene carbonate, EC and Propylene carbonate, PC) (T. Sakakura *et al.,* 2009).

CHAPTER III

LITERATURE REVIEW

3.1 Carbon dioxide removal

Proficient of carbon dioxide removal technology from industrial operations is an important part which has the potential to reduce the amount of carbon dioxide, as a greenhouse gas generated, to atmosphere. There are three basic groups of carbon dioxide capture methods, i.e. post-combustion capture, pre-combustion capture and oxy-fuel combustion (M. Wang et al., 2011). In post-combustion capture, CO_2 is captured from the flue gas obtained after the combustion of fossil fuel. In pre-combustion capture, the fossil fuel is fist reacted with air or oxygen before being partially oxidized to form CO and H_2 (known as syngas) and then, it is reacted with steam to produce a mixture of CO_2 and more H_2. The carbon dioxide is removed before combustion takes place. Oxy-combustion is when oxygen is used for combustion instead of air, which results in a flue gas that consists mainly of pure $CO_2$and is potentially suitable for storage. However, this study focused mainly on the post-combustion capture of CO2 method.

Nowadays, there are several post combustion gas separation and capture technologies using in natural gas treatment and carbon dioxide removal after the reactor, namely; (a) absorption,(b) cryogenic separation, (c) membrane separation and (d)micro algal bio-fixation (e) adsorption (A. Rao et al., 2002). Figure 3.1 summarizes various technology options for post combustion CO2 capture.

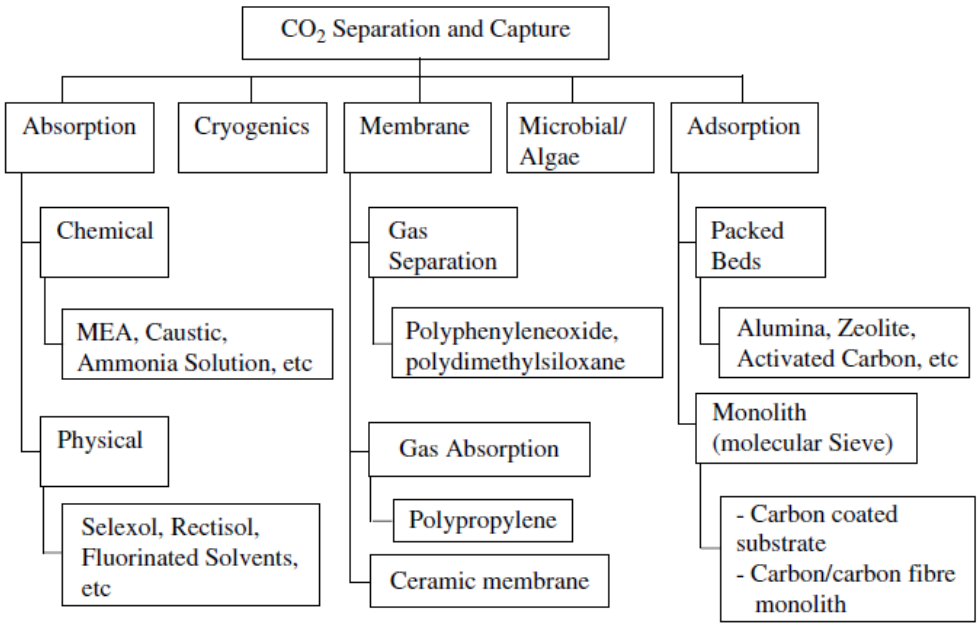

Figure 3.1 Different technologies for CO2 removal.

(R. Thiruvenkatachari et al., 2009)

Chemical absorption is one of the preferred methods for capturing CO2 at of low to moderate amount (3-20%) from post combustion flue gas streams (B.P. Sprgarelli *et al*., 2013). This is a well-known CO2 capture system widely used in the chemical and oil industries. Principle of chemical absorption of CO2 from gas mixture such as flue-gases is acid–base neutralization reactions using basic solvents (David J *et al*., 2000). Some of solvents for CO2 capture are amines (e.g. Monoethanolamine, MEA) (Ma'mun S.*et al*., 2007), ammonia solution (Bai H *et al*., 1997), Selexol (dimethylethers of polyetheleneglycol) (Chen C *et al*., 2003), Rectisol (chilled ethanol) (Rectisol H.G., 1970), fluorinated solvents (Heintz YJ et al., 2005) etc. The effluent gas is first cooled before being fed to the absorption column, where the basic solvent absorbs CO2 by chemical reaction. The CO2-rich solution from absorption column is fed to a stripper column where the temperature is increased (to about 120°C) in order to release the CO2 from the solvent (known as regeneration). The released CO2 is compressed and storage and the regenerated solvent solution is recycled to the stripper column. Figure 3.2 shows the basic flow diagram for CO2 capture by solvent absorption)

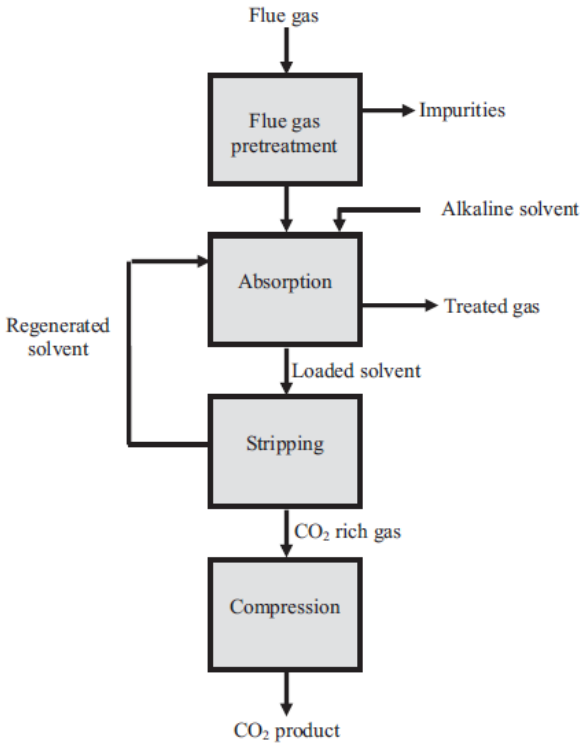

Figure 3.2 Basic flow diagrams CO2 capture using chemical absorption.

(B.P. Sprgarelli*et al.*, 2013)

3.1.1 Amine based solvent absorption

Amine absorption has been used widely by the natural gas industry to remove CO2 from natural gas. Amines react with CO2 to form water soluble compounds. Because of this compound formation, amines are able to capture a low to moderate CO2 partial pressure from gas mixture, but the efficiency is limited by chemical equilibrium. Amines are available in three forms (primary, secondary, and tertiary), each form comes with its advantages and disadvantages. In addition to options for the amine solvent, additives can be used to modify system performance. Finally, design modifications are possible to decrease capital costs and improve energy integration.

Amines could be classified as primary, secondary or tertiary based on the degree of substitution of the nitrogen atom. Monoethanolamine (MEA) consists of one alkanol chain and two hydrogen atoms bonded to a nitrogen atom and thus it is classified as a primary amine with the molecular formula (C2H4OH)NH2. Diethanolamine (DEA) consists of two alkanol chains and one hydrogen atom bonded to the nitrogen atom and is a secondary amine with the molecular formula (C2H4OH)2NH. Triethanolamine (TEA) is a tertiary amine (C2H4OH)3N as in the same way (Booth, 2005). However, there are various types of ethanolamine produced by replacing the ethanol groups with other hydrocarbons. Monodiethanolamine (MDEA) is a tertiary amine which one of the ethanol groups is replaced by methyl group (Booth, 2005).

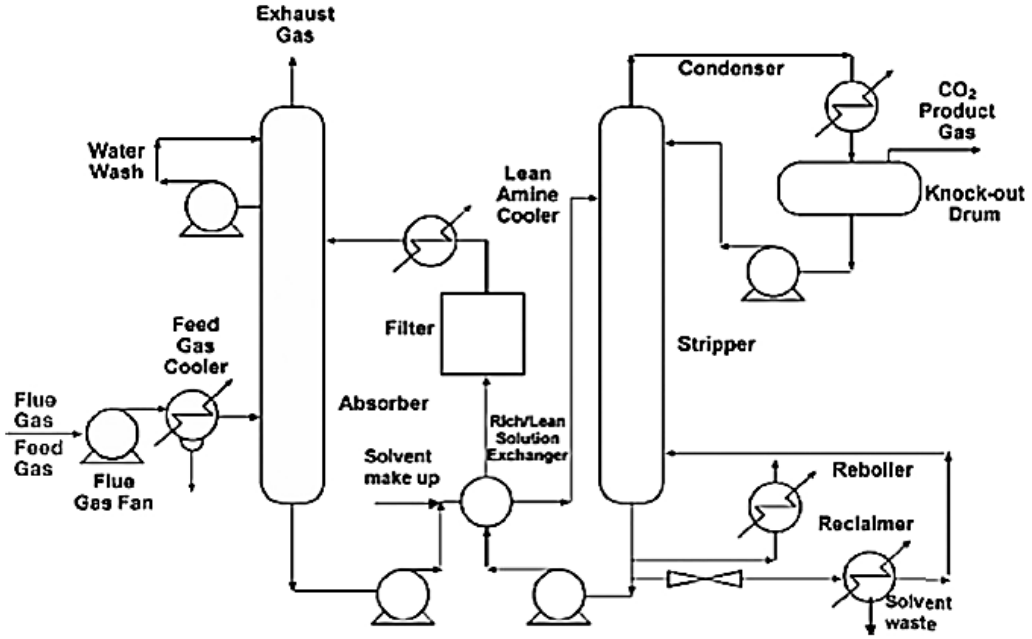

Figure 3.3 General process flow diagrams for amine absorption process (IPCC, 2005)

The conventional process of CO2 absorption by amine solution is displayed in Figure 3.3. The flue gas is fed in counter-current flow with the lean solvent into the absorber. The treated gas is then washed and went to storage. The rich solvent is

heated by the lean solvent from the stripper. The lean solvent is regenerated at raised temperature (100-120°C) to remove CO2 captured. Energy supplied to the reboiler is the major drawback of the process which is mainly concerned as the reason to select the proper absorbent.

Table 3.1 Properties of common amine solvents (adapted from T.E. Rufford et al., 2012)

Solvent	Monoethanolamine	Diethanolamine	Diglycolamine	Methyldiethanolamine
Acronym	MEA	DEA	DGA	MDEA
Solution concentration (wt%)	15-25	30-40	50-60	40-50
Acid gas pickup (mol acid gas/mol amine)	0.33-0.40	0.20-0.80	0.25-0.38	0.20-0.80
Stripper reboiler normal range (oC)	107-127	110-127	121-132	110-132
Heats of absorption of CO2 (kJ/mol)	84.4	71.6	83.9	58.8

Chemical properties of major amine solvents used are reported in Table 3.1. Primary amines and secondary amines are the very reactive with CO2 but their heat of regeneration are very high. On the other hand, tertiary amines have low reactivity compared with the others but heat of regeneration required is much lower (S. Mudhasakul*et al*., 2013). So, a suitable solvent for CO2 absorption has to be selected

appropriately, since Astarita (1983) reported that 50-70% of the capital cost for an amine absorption process was depended on the solvent recirculation rate and another 10-20% on the duty for regeneration.

In many cases, mixed amine solvents offer reduced solvent circulation rates and lower heat duties in the stripping stage. Idem and colleagues (2006), compared MEA to a blend of MEA/MDEA. Their results found that with the MEA/MDEA blend a modest decrease in circulation rate could be achieved along with a large decrease in the heat duty needed for stripping compared to the MEA system.

There are many researchers developed the process model for CO2 absorption by various type of amine solvents. J.M. Plaza et al., 2009 studied performance of 35wt% MEA solution by simulating process model in Aspen Plus®. Both the absorber and the stripper used RateSep™ to calculate effect of mass transfer rigorously. The simulated data were validated by the pilot plant model and the results were in good agreement. Solution of MEA 35wt% resulted in 90% CO2 capture. In addition, Y. Chen *et al*., 2012 compared the performance of blended amine solvent, which is a mixture of MEA and AMP (2-amino-2-methyl-1-propanol), with the single amine solvent. The Electrolyte non-random two liquid model was employed to fit the data. The simulation results are compared with the experimental data. CO2 recovery was obtained at 89.8% with the decrease in regeneration duty. However, S.Mudharskul*et al*., 2013 proposed the novel solvent namely a-MDEA which is a mixed solvent of Piperazine (PZ) and Methyldiethanolamine (MDEA). The Aspen Plus® was again used as the simulation program and the proposed flowsheet shown in Figure 3.4.

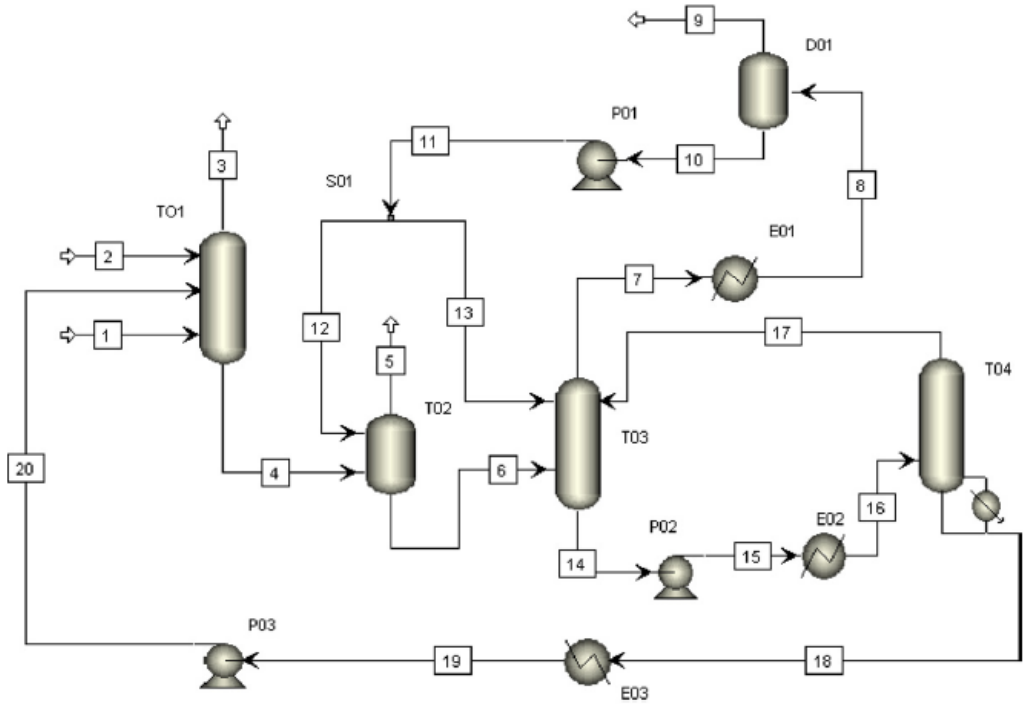

Figure 3.4 Process flow diagram of CO2 absorption process by a-MDEA (S.Mudharskul *et al.*, 2013)

Furthermore, the actual process data provided by the licensor of natural gas sweetening process plant in Thailand were used as the base case for simulation and were used to validate the model as well.

MDEA is, however, a tertiary amine that comes with relatively low reactivity to absorb carbon dioxide compared to other class of amine. Thus, an activator that could enhance the performance of reaction with CO2 has to be promoted in MDEA solution. Piperazine (PZ) was used in the studied and the mixed solvent is called activated-MDEA (a-MDEA). The novel solvent showed the outstanding performance. Effect of an addition of PZ was shown in Figure 3.5.

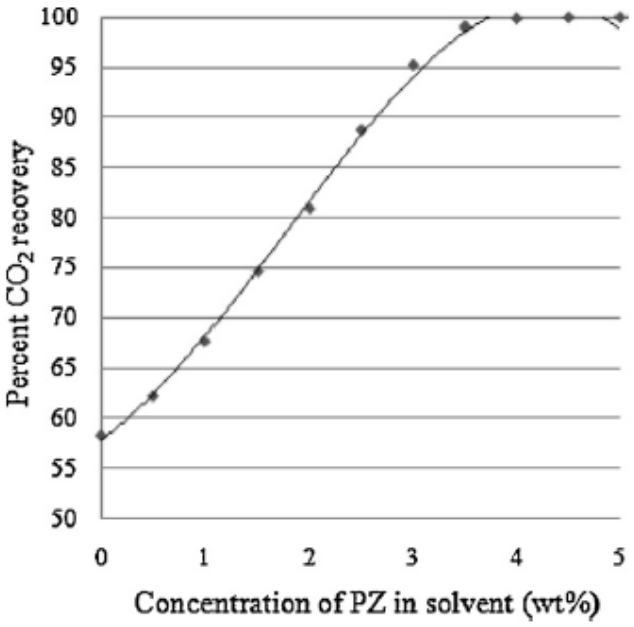

Figure 3.5 Effect of PZ concentration in MDEA solvent on CO2 recovery

(S.Mudharskul *et al*., 2013)

Optimal result reported as 5 wt% of PZ added to 45 wt% MDEA solvent which led to a hundred percent of CO2 capture and required duty regeneration of74.66 kJ/molCO2, which is much lower than other types of amine absorbent.

3.2 Oxidative Coupling of Methane (OCM)

3.2.1 Catalysts and reactor

Most of chemical reactions may have undesired side reactions which led to low production yield from the main reaction. OCM is known as one of many reactions that come with complex reaction network. Side reactions of OCM such as partial oxidation to H_2 and CO or complete oxidation to CO_2 and H_2O are resulted in decrease of C2 yield and selectivity. Worldwide researchers have dedicated to develop efficient catalysts such as oxygen capacity on surface catalyst, catalyst activity, and catalyst stability for this reaction system. Main interest of the research on the reaction was to look for a more active catalyst to increase C_2 hydrocarbons production. Various types of reactors such as fixed bed reactor, membrane reactor

and SOFC reactor have been reported for OCM reaction. Most reported studies on OCM were carried out in fixed-bed reactors in co-feed operation mode because it was easiest to design but this reactor presented the low C_2 yield. These systems also have another application as a membrane reactor for selective oxidation. Figure 3.6 shows configuration of two mentioned reactors.

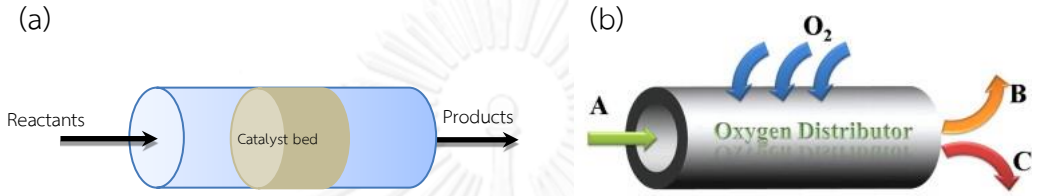

Figure 3.6 Configuration of; (a) fixed bed reactor, (b) membrane reactor

In a fixed-bed reactor, catalysts are held in place and do not move with a fixed reference frame. The reactor was operated by co-feeding of methane and oxygen through the catalyst bed. The OCM reaction takes place on the surface of the catalyst. Generally, OCM reaction occurred at temperature of 873-1273 K. Most researches about OCM reactor emphasized development of the catalyst performance to increase methane conversion and C_2 selectivity at the same time. Many catalysts have been studied and promised to be effective catalysts for OCM reaction. Rare earth oxide catalysts (La_2O_3, CeO_2, Sm_2O_3) provided a high performance for this reaction. Rane*et al*., (2008) reported alkali metal promoted on CaO in OCM reaction, the experimental result exhibited increasing in the surface basicity and the C_{2+} selectivity and yield of the catalysts in the OCM process. Murata *et al*., (1998) investigates Li-doped sulfated-zirconia catalysts and it was found to be effective for oxidative coupling of methane. In addition, alkaline-earth-metal fluoride such as SrF_2-La_2O_3, SrO-LaF_3, BaF_2-CeO_2 showed good catalytic performance in OCM. Chao *et al*., (1995) studied on BaF_2/LaOF in fixed-bed quartz reactor at atmospheric pressure. Catalyst had CH_4 conversion of 33.08% and a C_2 selectivity of 62.47% was achieved at CH_4:O_2 = 3:1. The best OCM reaction results were obtained over BaF_2/LaOF with BaF_2 content in 10 to 18 mol%.

There are other interesting options of a few transition metal oxides that contain Group IA ions or transition metal-based catalyst, for example, $Mn/Na_2WO_4/SiO_2$. Jiet *al*., (2002, 2003) have the great attention in the Na_2WO_4-Mn/SiO_2 catalyst system because of its excellent catalytic performance. They are proposed the relationship among structure and the performance of Na-W-Mn/SiO_2 catalysts. It was found that Na-O-Mn and Na-O-W species is an active site and suitable percent contain of Na=0.4–2.3%, W=2.2–8.9%, and Mn=0.5–3.0%. Recently, Liu *et al*., (2008) scale up and stability test for oxidative coupling of methane over Na_2WO_4-Mn/SiO_2 catalyst the highest C_2 (ethylene and ethane) yield of 25% was achieved. When increased temperature from 913 to 1073 K the C_2 yield decreased and the CO_x certainly increased. The same catalyst was studied by Wang *et al*., (1995) and they suggested that Na–W–Mn species were the most probable active sites, in which Mn was an active component, Na was required for high selectivity, and W ions were required to stabilize the catalyst.

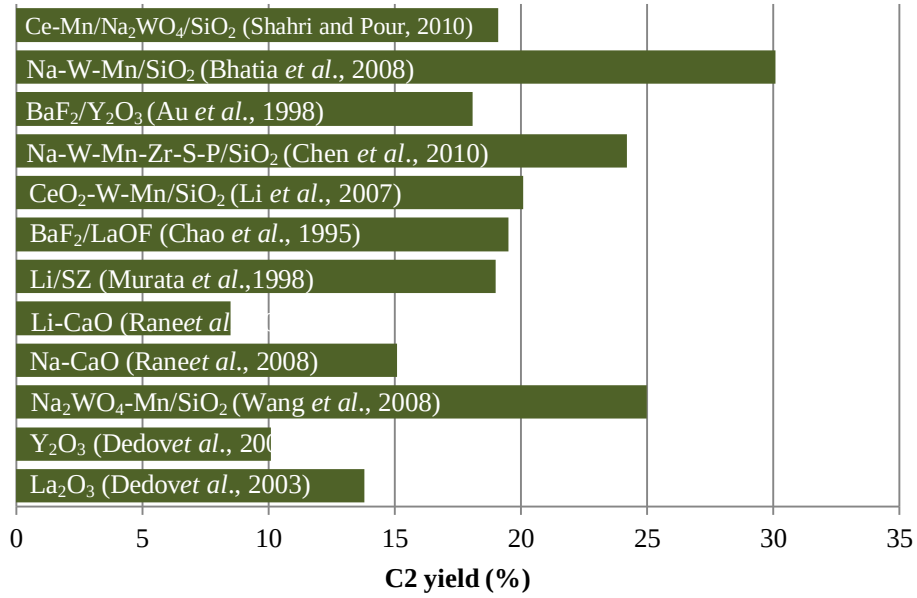

Figure 3.7 Performance of OCM catalyst in literature review

In comparison, Na-W-Mn/SiO_2 showed better performance than other OCM catalysts. Both Na-O-Mn and Na-O-W acted as the active centers of the catalysts for

OCM. Figure 3.7 shows the performance of catalyst in literature review. Although, there are problems in fixed bed reactor that would be taken into account; (1) the oxygen species is one of main problem to study because in co-feeding, the partial oxidation and the complete combustion can be occurred, which led to lower C_2 selectivity and yield; (2) OCM is known as the highly exothermic reaction, therefore, the hot-spot problem which resulted in increasing of temperature inside the reactor and might be a reason for side reaction taking place which led to lower C2 yield and selectivity.

To solve problems of fixed bed reactor, membrane reactor was applied to the oxidative coupling of methane process. The membrane reactor could be classified into three main categories according to the mechanism of transportation for oxygen specie; (1) porous membrane, which oxygen molecule transport into the pores; (2) dense membrane, which oxygen lattice diffusion is occurred; and (3) dense oxygen ionic conducting solid oxide electrolyte membrane, which oxygen molecule is transported by ion conduction mechanism (Liu et al., 2001). However, for OCM process in industrial scale, the use of dense membrane is difficult to be applied due to high selectivity of membrane, which is non-permeable for other components except oxygen, led to low permeation rate and low reaction rate compared to the other types of membrane reactor. Therefore, porous membrane reactor is recommended to apply for industrial OCM process (S. Stunkel et al., 2009).

The porous membrane is a complementary of ceramic materials such as **α**-alumina, ZrO2, TiO2, CaO and Vycor glass (Liu et al., 2001). Among those choices of materials, **α**-alumina shows higher stability at high temperature and therefore usually preferred. Porous membrane is operated based on the following five different mechanisms respectively; (1) Knudsen diffusion, (2) surface diffusion, (3) capillary condensation, (4) laminar flow and (5) molecular sieving. Based on most studies of membrane permeable measurement and membrane characteristic, the oxygen transport through the membrane is usually conformable of Knudsen diffusion

phenomena (Zaman J. et al., 1994, Lafarga D. et al., 1994) and could be expressed by the following equation (Saracco G. et al., 1994).

$$J_i = \frac{G\Delta P}{L(2M_i RT)^{0.5}} \quad (3.1)$$

Ji Permeation flux of component (i), mol/cm2/s

G Geometric factor of membrane

P Gas partial pressure, atm

L Membrane thickness, cm

Mi Molecular weight of component (i), g

R Gas constant

T Temperature, K

Results of OCM in the various type of porous catalytic membrane reactor are reported in Table 3.2.

Table 3.2 Performance comparison of OCM in various porous membrane reactors

Membrane	Catalyst	T (oC)	C2 yield	C2 selectivity	References
LaOCl-alumina	LaOCl	750	8.90%	-	Julbe et al, 1991
Silica-alumina	Li/MgO	750	22.50%	-	Coronas et al, 1994
LaOCl-alumina	LaOCl	750	11%	-	Borges et al, 1995
Vycor tube	Sm2O3	750	10.50%	33.00%	Ramachandra et al, 1996
a-alumina coated with amorphous Sit 2	Sm2O3 doped with MgO	700	3.00%	23.00%	Tonkovich et al., 1996
Silica-alumina	Li/MgO	690	24%	-	Coronas et al, 1997
Y-alumina	Mn-W-Na/SiO2	810	27.50%	-	Lu et al, 1999
Porous alumina	La/MgO	850	9%	-	Kanno et al, 2000
a-alumina from MKS co.ltd	La/MgO	900	7.41%	13.00%	Lafarga et al., 2001
a-alumina support, y-alumina	Li/MgO	750	30%	53%	Kao et al., Coronas et al., 2003
a-alumina support, y-alumina (Membralox)	Li/MgO	900	44%	85%	Kiatkittipong et al., 2005

For the performance of membrane reactor compared with conventional packed bed reactor in terms of temperature profiles in the catalyst, stability of the reactors, effect of reactor configurations on selectivity, conversion, and C2 yields, it could be concluded that the membrane reactor allows a more controllable (ease of avoidance of hot spots) and safer (decrease the possibility of an explosion) operation and gives a considerably better selectivity, especially at low and moderate methane and oxygen conversions (Coronas et al., 1994).

3.2.2 Mechanisms and kinetic

As seen from the previous reports about the performance of OCM on various kinds of catalyst, Na-W-Mn/SiO2 shows the outstanding catalytic activity for OCM reaction. Therefore, OCM rate expression and reaction kinetic for Na-W-Mn/SiO2 was focused particularly in this research.

More in detail about OCM kinetic expression, there were many researchers had studied and suggested the OCM reaction network over a variety of catalysts, i.e., La2O3/CaO (Z. Stansch et al., 1997), CaTiO3 (M. Sohrabi et al., 1996), La2O3 (S. Lacombe et a., 1995), BaCO3/La2On(CO3)3-n (U. Olsbye et al., 1992), La2O3/MgO (M. Traykova et al., 1998) and Mn/Na2WO4/SiO2 (S.M.K. Shahri et al., 2009). The reaction network of those models was concluded in Table 3.3.

M. Daneshpayeh et al., 2009 proposed the kinetic model of Na-W-Mn/SiO2 derived from the above reaction networks. Stansch's model with nine heterogeneous catalytic reactions and one homogeneous gas phase reaction properly fitted with their experimental results; therefore, the kinetic parameters were calculated by statistical model fitting methodology which resulted in 9.15% average absolute relative deviation (AARD) and R^2 of 0.964 respectively. The kinetic model and parameters were reported in Table 3.4.

Table 3.3 OCM reaction network proposed by researchers

	Reactions	Stansch et al. 1996	Sohrabi et al. 1996	Lacombe et al. 1995	Olsbye et al. 1992	Traykova et al. 1998	Shahri et al. 2009
1	$2CH_4+0.5O_2 \rightarrow C_2H_6+H_2O$	✓	✓	✓	✓	✓	✓
2	$CH_4 + O_2 \rightarrow CO + H_2O + H_2$	✓			✓		
3	$CH_4+1.5O_2 \rightarrow CO + 2H_2O$		✓			✓	✓
4	$CH_4+2O_2 \rightarrow CO_2 + H_2O$	✓	✓	✓	✓		✓
5	$2CH_4+O_2 \rightarrow C_2H_4+2H_2O$		✓				
6	$CO + 0.5O_2 \rightarrow CO_2$	✓		✓			
7	$C_2H_6 + 0.5O_2 \rightarrow C_2H_4 + H_2O$	✓		✓		✓	✓
8	$C_2H_6+O_2 \rightarrow 2CO+3H_2$			✓			
9	$C_2H_6+2.5O_2 \rightarrow 2CO+3H_2O$				✓		
10	$C_2H_6+3.5O_2 \rightarrow 2CO_2+H_2O$			✓	✓		
11	$C_2H_6 \rightarrow C_2H_4 + H_2$	✓			✓	✓	
12	$C_2H_4+O_2 \rightarrow 2CO+2H_2$			✓			
13	$C_2H_4 + 2O_2 \rightarrow 2CO + 2H_2O$	✓			✓		✓
14	$C_2H_4+3O_2 \rightarrow CO_2+2H_2O$				✓		
15	$C_2H_4 + 2H_2O \rightarrow 2CO + 4H_4$	✓					
16	$CO_2 + H_2 \rightarrow CO + H_2O$	✓				✓	✓
17	$CO + H_2O \rightarrow CO_2 + H_2$	✓				✓	✓

Table 3.4 Kinetic model of OCM reaction proposed by M. Daneshpayeh et al., 2009

$$r_1 = \frac{k_{01} e^{\frac{-E1}{RT}} (K_{0,O2} e^{\frac{-\Delta Had,O2}{RT}} p_{O2})^{n1} p_{CH4}^{m1}}{\left[1+(K_{0,O2} e^{\frac{-\Delta Had,O2}{RT}} p_{O2})^{n1}\right]^2} \quad (3.2)$$

$$r_j = k_{0j} e^{\frac{-Ej}{RT}} p_C^{mj} p_{O2}^{nj} \qquad \text{j = 2-6} \quad (3.3)$$

$$r_7 = k_{07} e^{\frac{-E7}{RT}} p_{C2H4}^{m7} p_{H2O}^{n7} \quad (3.4)$$

$$r_8 = k_{08} e^{\frac{-E8}{RT}} p_{C2H6}^{m8} \quad (3.5)$$

$$r_9 = k_{09} e^{\frac{-E9}{RT}} p_{CO2}^{m9} p_{H2}^{n9} \quad (3.6)$$

$$r_{10} = k_{010} e^{\frac{-E10}{RT}} p_{CO2}^{m10} p_{H2O}^{n10} \quad (3.7)$$

	Reactions (from Stansch's model)	k_{0j} mol g^{-1} s^{-1} $Pa^{-(m+n)}$	$E_{a,j}$ kJ/mol	K_{O2} Pa^{-1}	$\Delta H_{ad,O2}$ kJ/mol	m_j	n_j
1	CH_4+2O_2 -> $CO_2 + H_2O$	2.94×10^{1}	212.6	4.39×10^{-11}	-121.9	1	0.75
2	$2CH_4 + 0.5O_2$ -> $C_2H_6 + H_2O$	3.07×10^{-7}	98.54			0.85	0.5
3	$CH_4 + O_2$ -> $CO + H_2O + H_2$	6.65×10^{-8}	146.8			0.5	1.57
4	$CO + 0.5O_2$ -> CO_2	5.26×10^{-4}	114.6			0.5	0.5
5	$C_2H_6 + 0.5O_2$ -> $C_2H_4 + H_2O$	2.70×10^{-3}	153.5			0.91	0.5
6	$C_2H_4 + 2O_2$ -> $2CO + 2H_2O$	1.81×10^{-1}	174.4			0.72	0.40
7	C_2H_6 -> $C_2H_4 + H_2$	4.61×10^{2}	394.2			1.62	0.71
8	$C_2H_4 + 2H_2O$ -> $2CO + 4H_4$	1.08×10^{7} [a]	291.9			0.88	0
9	$CO + H_2O$ -> $CO_2 + H_2$	5.77×10^{-3}	158.0			1	1
10	$CO_2 + H_2$ -> $CO + H_2O$	5.24×10^{-6}	131.3			1	1

[a] Units are mol s^{-1} m^{-3} Pa^{-1}

3.3 Direct oxidation of ethylene

3.3.1 Catalysts

Several metal type catalysts were studied for direct oxidation of ethylene. H. Nakatsuji et al., 1995 reported the activation of oxygen on copper, silver and gold surfaces and three catalysts showed similar results. S. Rojluechai et al., 2007 studied this reaction on supported gold and silver catalysts and found that the activity was favor to generate ethylene oxide. They also performed a study on Au/TiO2 and resulted in higher selectivity of ethylene oxide but lower conversion compared to silver catalyst. A. Carvalho et al., 2007 studied in further about the performance of Cs-promoted and non-promoted silver catalyst. They found that Cs-promoted one increased ethylene oxide yield but still had problem about stability and selectivity. The reaction was studied in microreactor system by Kestenbaum et al. in 2002. They use polycrystalline silver plates without support as catalyst. The experiments were carried out by varying concentration of feed, total gas flow rate and pressure. The results were obtained that selectivity of ethylene oxide depended on partial pressure of oxygen and achieved at 50%. Ethylene oxide yield increased with increasing oxygen pressure together with a slight increase in conversion. In addition, the catalyst was maintained at 1000 hours without any deactivation.

3.3.2 Mechanisms and kinetic

There have been various kinetic model proposed to describe the experimental results. Petrov et al., 1988 used silver on a-alumina support promoted by Ca in a circulation flow system. They considered a single-site Eley-Rideal proposed mechanism to explain and reported similar rate equations of both selective oxidation and complete combustion reactions. The model was described in (3.8) and (3.9).

$$r_1 = \frac{k_1 p_E p_O}{1+K_E p_E p_O} \tag{3.8}$$

$$r_2 = \frac{k_2 p_E p_O}{1+K_E p_E + K_O p_O} \tag{3.9}$$

In 1983, Ghazali et al., using a fixed-bed semi-differential reactor at low temperature. Later in 1987, Park and Gaul studied in further detail and found that the catalyst surface was partly covered by carbonaceous deposits, therefore, a dual-site Langmuir-Hinshelwood mechanism was used to represent the data and the following rate equations were proposed.

$$r_i = \frac{kK_E K_O p_E p_O}{(1+K_E p_E+K_O p_O+K_{EO} p_{EO})^2} \tag{3.10}$$

Based on Langmuir-Hinshelwood mechanism, Borman and Westerterp (1995) presented the model which all partial pressure of the components were taken into account, by using an industrial-available Ag/a-Al2O3 catalyst in an internal recycle reactor, the following expression was reported.

$$r_i = \frac{k^i K_E^i \sqrt{K_O^i} p_E \sqrt{p_O}}{(1+K_E^i p_E+\sqrt{K_O^i p_O}+K_C^i p_c+K_W^i p_W+K_{EO}^i p_{EO})^2} \tag{3.11}$$

Larfaga et al., 2000 studied the reaction over Cs-doped silver catalyst on a-Al2O3 pellets support in a differential reactor. The previous models available in literature were taken into consideration and the simplified kinetic model based on Langmuir-Hinshelwood mechanism was reported.

$$r_i = \frac{k^i p_E p_O^{ni}}{(1+K_E^i p_E)^2} \tag{3.12}$$

Hernandez C. et al., 2010 proposed two kinetic models in order to fit their experimental data. The first model assumed that ethylene and oxygen adsorbed competitively on the catalyst surface. The second model assumed competitive adsorption of ethylene and oxygen molecule on the surface. Both two models assumed that surface reaction was rate limiting step. They found that the second model was slightly better fitted their data.

$$r_i = \frac{k' C_E C_O}{(1+K_E C_E+K_O C_O)^2} \tag{3.13}$$

Recently in 2012, A. Peschel et al. proposed a study of plant wide optimization for ethylene oxide process in which the kinetic model of Gan et al. (2001) was applied. The kinetic model was described in the following equations:

$$r_1 = \frac{k_1(T)p_E p_O}{1+K_1(T)p_O+K_2(T)p_O^{0.5}p_{CO2}} \quad (3.14)$$

$$r_2 = \frac{k_2(T)p_E p_O^{0.5}}{1+K_1(T)p_O+K_2(T)p_O^{0.5}p_{CO2}} \quad (3.15)$$

$$k_1(T) = \exp(-4.087 - \frac{43585.7}{RT}) \quad (3.16)$$

$$k_2(T) = \exp(3.503 - \frac{77763.2}{RT}) \quad (3.17)$$

$$K_1(T) = \exp(\frac{18321.0}{RT} - 16.644) \quad (3.18)$$

$$K_2(T) = \exp(\frac{34660.6}{RT} - 14.823) \quad (3.19)$$

3.4 Process intensification of OCM

Although there are many researches about the activity of catalysts on OCM performance but the selectivity and yield of C2 products were still limited and the economics of the process were not attractive. Therefore, many researches have been switched to the process design topic (J.A. Hugill*et al*., 2005). There was a research study from J.A. Hugill*et al*., 2005 dedicated their effort to develop the co-generation of ethylene and electricity process. The co-generation process scheme suggested by Swanberg (1998) is shown in Figure 3.8.

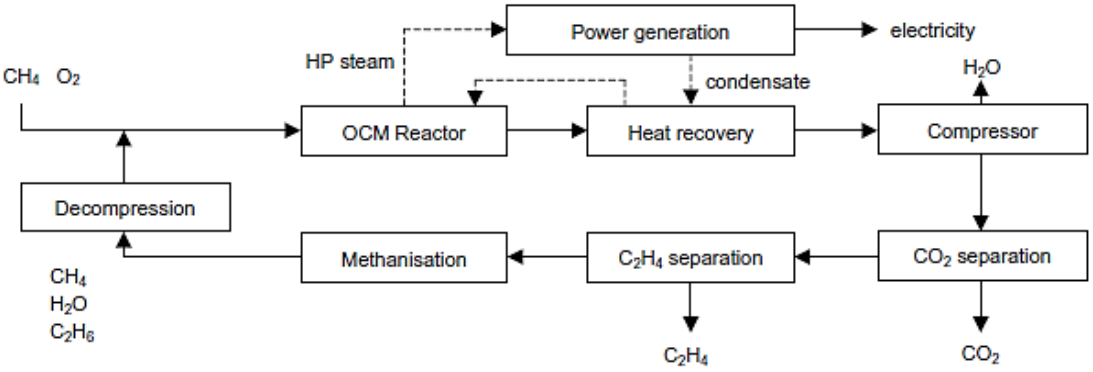

Figure 3.8 Process scheme of co-generation process (Swanberg, 1998)

The proposed scheme suggested that utilizing heat of OCM reactor, which is the highly exothermic; to generate electricity could be resulted in better process performance. In addition, the co-generation process was compared with the individual production of ethylene and electricity plant. The cost comparison was analyzed based on the exergy analysis suggested by J. Szargut*et al*., 1988. However, the results were reported that; in case of CO2 emission, the co-generation process reduced CO2 emission significantly but; in case of energy saving and costs, the co-generation process had lower profitability compared to the conventional process of ethylene and electricity production. Their results are shown in

Table 3.5.

Table 3.5 Performance of the co-generation process compared with the conventional process

Exergy use	Ethylene production	Electricity generation	Ethylene + Electricity plant	Co-generation	Co-gen advantage (%)
Fuel	74	109	183	189	-3
Feedstock	158	0	158	168	-6
Fuel + Feedstock	233	109	342	357	-5
CO2 emission					
CO2 production (t/h)	17	17	34	29	13
Exergy use (MW)	74	87	161	189	-17
CO2/exergy (kg/GJ)	62	53	57	42	26

Costs	IRR (%)	
	10-year project	25-year project
Separate generation	19	22
Co-generation	0.18	8.5

D. Salerno et al., (2011) proposed the integration of ethylene and methanol production process. The motivation of this work was to utilize the unreacted methane form OCM, so, the alternative process for methanol production and the co-generation of electricity was designed in order to make the overall process to be economically attractive and also designed for industrially implementation. The methanol production process is shown in Figure 3.9.

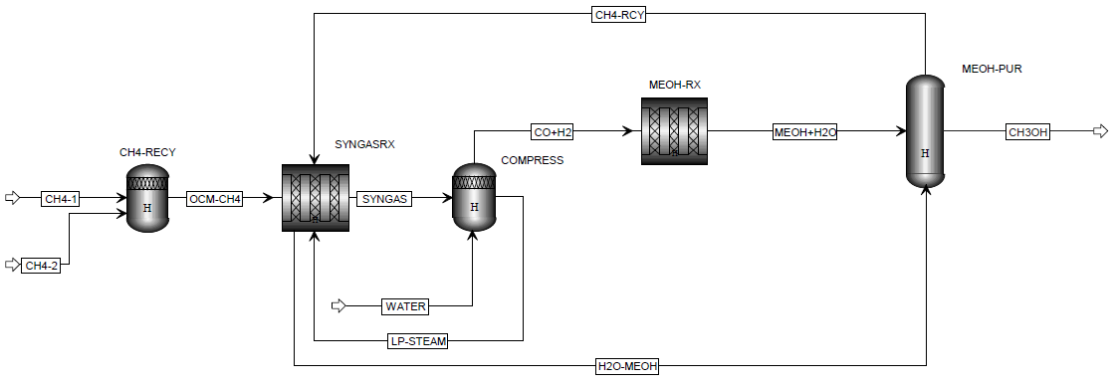

Figure 3.9 Alternative methanol production process using unreacted methane from OCM (D. Salerno et al., 2011)

Total project investment cost was calculated based on total equipment cost, variable and fixed operating cost which was developed based on material and energy balance taken from simulation results. The simulation results were summarized in Table 3.6 and total investment cost was calculated and reported in Table 3.7 respectively.

Table 3.6 Mass flow rates of the key components from process

Raw materials	*Ton/day*
Methane	652
Oxygen	433.5
Products	
Methanol	356.2
Methanol purity (wt%)	99.9
Electricity (kW)	4019.1
Byproducts	
H2O	351.6
CO2	94.3
CO	1147.9
H2	101.3
Unreacted CH4	519.2

Table 3.7 Capital cost for the proposed process

Process section	Price ($x10^6$ EUR)
Methane conditioning	7.45
Methane and Syngas POX	11.98
Gas compressing	33.05
Methanol reaction	5.44
Methanol purification	7.17
Total installed equip. cost	65.09
Total direct and indirect cost	82.08
Contingency	14.77
Fixed capital investment	96.86
Working capital	14.53
Total captital investment	111.38

The study reported that it is possible to produce methanol from the effluent of OCM process. The alternative production process of valuable chemical such as methanol increases value to the OCM process beside the ethylene production and natural gas utilization. In addition, the payback period was expected to be approximately 4 years. For 20-years project, the results showed that the suggested process scheme was able to imply in industrial scale.

Later in 2012, D. Salerno et al. again proposed the additional section of formaldehyde production in their alternative methanol production form OCM process. The unreacted methane was selectively oxidized to be formaldehyde in this study. The main reason was the amount of CO generated from OCM reaction was too attractive to be sold as byproduct. Therefore, CO generated was designed to use in the synthesis gas production for adjusting the ratio of H2 and CO to be suitable for methanol production. Figure 3.10 displayed the process diagram.

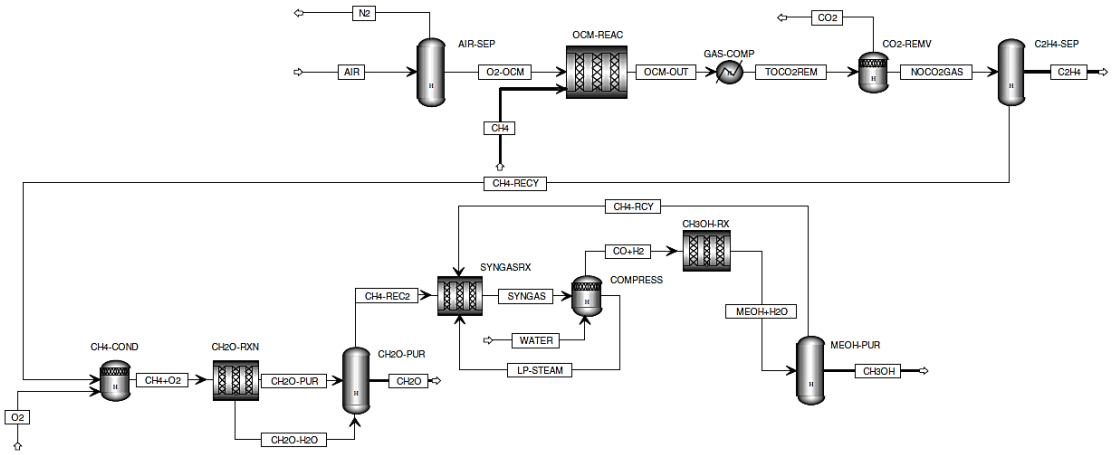

Figure 3.10 Process flow diagram of formaldehyde and methanol production process (D. Salerno et al., 2012)

The simulation results and the economic analysis were obtained and were compared with the results of conventional OCM process. Table 3.8 summarized the flow rates of two processes and Table 3.9 showed the comparison of economic results respectively.

Table 3.8 Simulation results of OCM and proposed process

	Conventional OCM	Proposed process
Raw materials	*Ton/day*	*Ton/day*
Methane	2593.2	652
MEA	676.7	433.5
Products		
Ethylene	396	396
Ethylene purity (wt%)	99.6	99.2
Formaldehyde	-	117.1
Methanol	-	204.2
Byproducts		
H2O	1438.9	29.2
C2H6	19.6	25.7
CO2	1675.2	518.8
CO	126.5	1512.9
H2	72	108.6
Unreacted CH4	1421.1	502.2

Table 3.9 Economical analysis comparison of two processes

Investment (x106 EUR)	Conventional	Proposed process
Total project capital cost	170.67	183.94
Total operating cost	266.05	255.34
Total raw material cost	83.77	81.31
Total utility cost	154.89	147.71
Total product sales (C2H4)	272.4	272.4

The analysis showed that it was possible to produce ethylene also formaldehyde and methanol from the unreacted methane. The payback period was approximately 8 years for this project. Ethylene produced was suitable to satisfy the ethylene demand in worldwide market, as a feedstock for chemical production.

Recently, H.R. Godini et al. (2013) performed techno-economic analysis of the combination process of OCM and dry methane reforming. At first, they analyzed the detailed of fixed- and operating cost of the standalone OCM process in order to identify the economical attractive of the process. The designed process is shown in Figure 3.11 and the detailed cost evaluation obtained by Aspen Economy Analyzer® is reported in Table 3.10 and Table 3.11.

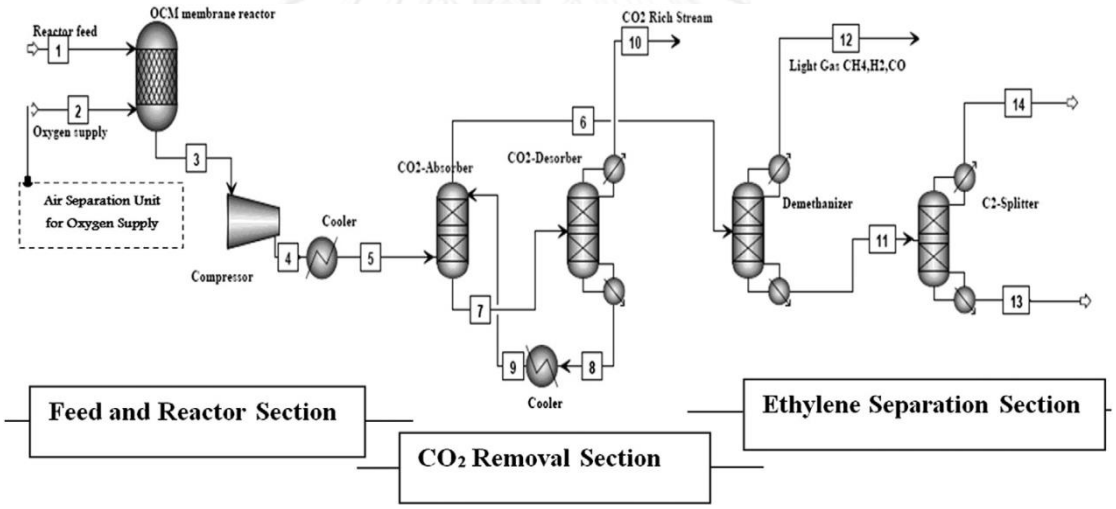

Figure 3.11 The original OCM process scheme (H.R. Godini et al.,2013)

Table 3.10 Detail of total project capital cost for OCM process

Cost of each OCM process section	Capital (mill.EUR)
Equip. in air separation unit	19.7
Reactor and corresponding equip.	11.6
CO2 removal section	38.3
Ethylene separation	9.8
Total direct and indirect cost	122.3
Contingency	22.1
Working capital	22.8
Total project capital cost	151.7

Table 3.11 Utility cost in different sections of OCM process

Sections	Utility cost (mill.EUR/year)	Note
Air separation	63.2	Electricity for compression and cooling
Reactor section	14.7	Complementary heating of the reactor feed
Gas compression	74.7	Electricity for compression and cooling
CO2 removal section	46.5	Pump, regenerator and reboiler duties
Ethylene separation	27.5	Electricity for compression and cooling

As shown in Table 3.10 and Table 3.11, for the 250,000 MT per year of ethylene production, the authors reported that the fixed cost of CO2 removal section and utility for gas compression are the major investment of the process due to the large amount of gas flow rate which required large equipment to operate. Furthermore, total operating cost and utility cost per year are 254 and 228.6 million Euro and required energy of 63 gigajoules for a ton of ethylene production. Thus, the standalone OCM process became uneconomic compared to the conventional ethylene production, which is the naphtha cracking process.

In order to increase the economic potential of the process, methane reforming section was integrated to the original OCM process, as shown in Figure 3.12, so as to utilize the exothermic heat from OCM reactor by supplying to the methane reformer in which the endothermic reaction is occurred.

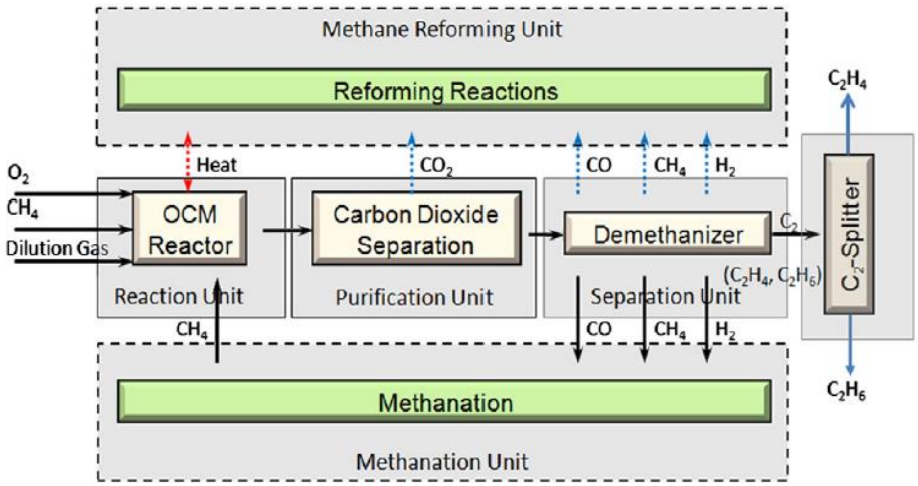

Figure 3.12 The proposed process in which the methane reformer was integrated.

The authors suggested more about schemes of integrating process shown in Figure 3.13. The first one (Figure 3.13 (a)) was designed based on the original OCM process which utilized heat form OCM reactor supplying to methane reformer with the effluent from OCM including CH4, CO, H2 and especially CO2. For the case of using adsorber (Figure 3.13 (b)), the adsorption by Zeolite 4A was introduced to separate CO2 and C2 from other components. The CO2 remaining, together with other components, were then utilized by dry methane reforming reaction.

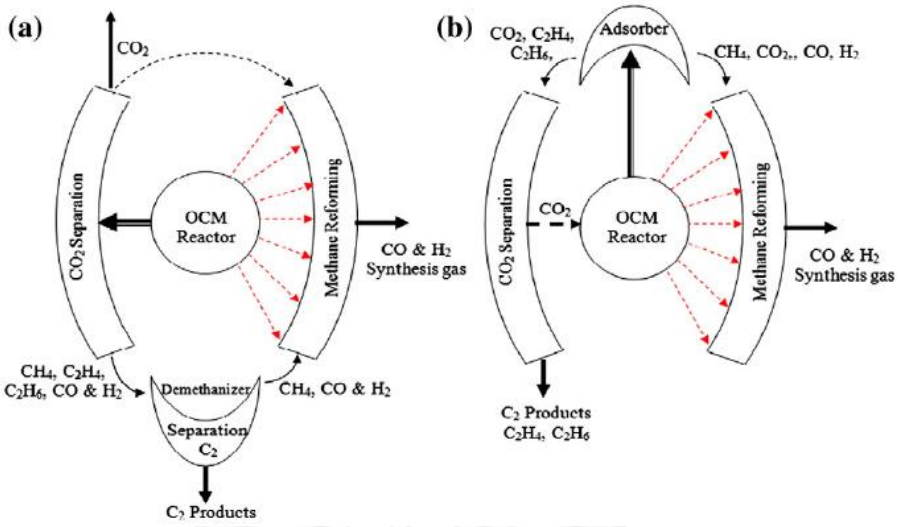

Figure 3.13 The proposed schemes of integrating process; (a) based on original OCM process and (b) based on alternative OCM process in which the adsorber was involved

However, from the results, the authors concluded that the scheme with adsorber involved was not a proper choice because of the ethylene loss into the reformer, which was limited by the selectivity of Zeolite 4A adsorbent. Thus, the integrated model based on the original one was continued on the study and performance of the proposed process was reported in Table 3.12.

Table 3.12 Performance of the integrated process

OCM membrane reactor	
Methane conversion for OCM	46.38%
C2 yield for OCM	36.23%
Heat realeased from OCM	12.48 W
DRM fixed bed reactor	
Methane conversion for DRM	26.07%
Heat consumed from DRM	4.83 W
Overall process	
Overall methane conversion	60.36%
Overall C2 yield	35.86%
Overall heat rate (released)	7.65 W

In summary, integrating of OCM and DRM process is a promising concept for utilizing CO2 generated together with unreacted methane as reactants for dry methane reforming reaction which can increase the process economy compared to the standalone OCM process.

CHAPTER IV

PROCESS SIMULATION

In this chapter, steps and methods of ethylene carbonate production process from wheat straw were discussed. The overall process and process description were also explained in this chapter.

4.1 Process description

The overall process was divided into four sections including the biogas production and treatment, the OCM process, the EO production and the EC production as shown in Figure 4.1.

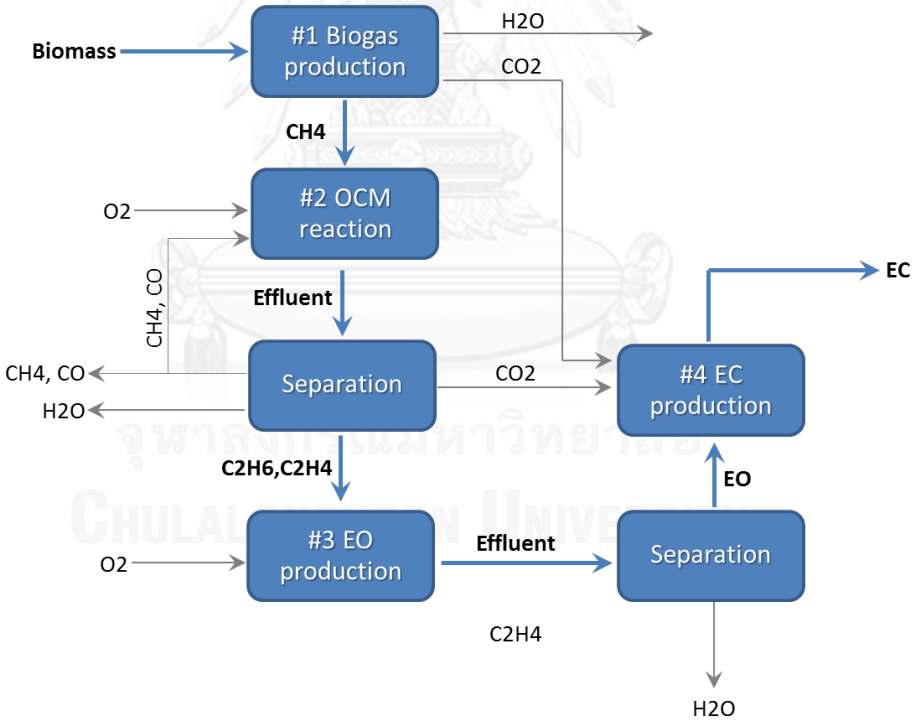

Figure 4.1 Overall process scheme

Wheat straw, as the biomass feedstock for this process, was fed to produce biogas (stream 1-1) via the anaerobic digestion process as reported by M. Shafiei et al, 2013. The composition of biogas produced (stream 1-2) consisted mainly of carbon dioxide, methane and water vapor. Biogas was then treated CO2 by the chemical absorption process of MEA solution (stream 1-4) followed by removing of water vapor by physical condensation. Treated gas, called bio-methane (stream 1-12), was fed to OCM section and carbon dioxide consisted in biogas (stream 1-7) was fed to section #4 to produce ethylene carbonate afterward. The aforementioned process was named as the section #1 of the overall process and was depicted in Figure 4.2 respectively.

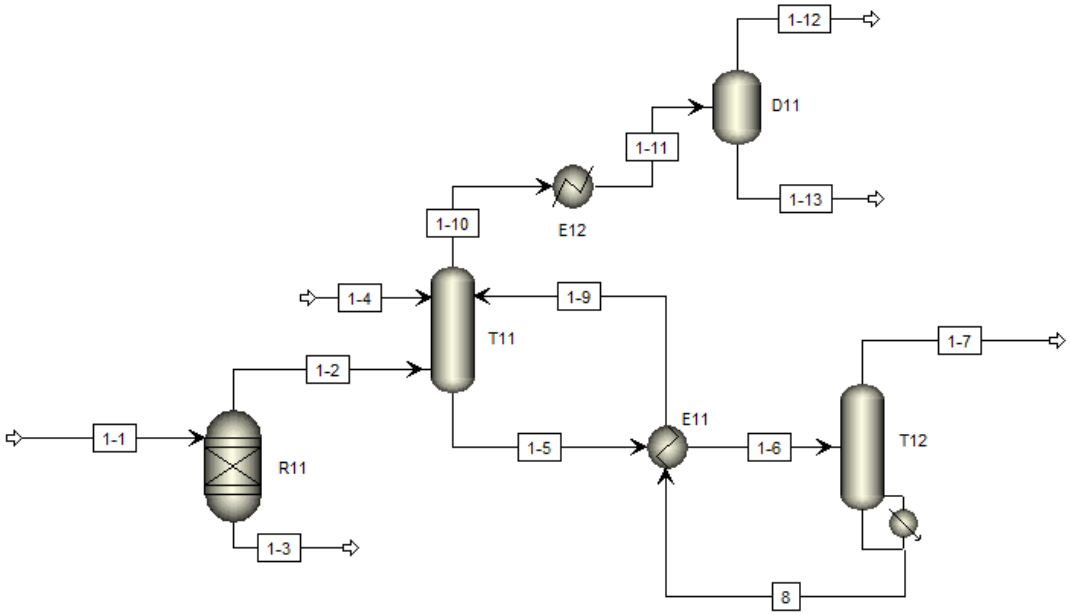

Figure 4.2 Biogas production and treatment (Section #1).

Bio-methane from previous section was fed together with oxygen (stream 2-1) as reactants for OCM reaction. Gas mixture (stream 2-2) was heated to 850°C before entering the reactor. OCM reaction took place on Na-W-Mn/SiO_2 catalyst packed inside the tubular reactor. Effluent from the reaction, which consisted of ethane, ethylene, carbon dioxide, carbon monoxide, hydrogen, water and the remaining of methane and oxygen, was cooled down before entering the CO2 absorption process

by MEA solution (stream 2-22) followed by removing of water vapor by physical condensation. Mixed C2 (ethane and ethylene, stream 2-17) was separated from gas mixture by distillation tower (T23) in the same way as methane was separated from light gas (T24). Methane remaining (stream 2-19) was recycled and mixed with bio-methane and oxygen while light gas remaining (hydrogen, oxygen, carbon dioxide and carbon monoxide, stream 2-18) was purged from the process to prevent the accumulation and treated carbon dioxide (stream 2-9) was fed to EC production section. Process scheme for section #2 was shown in Figure 4.3 respectively.

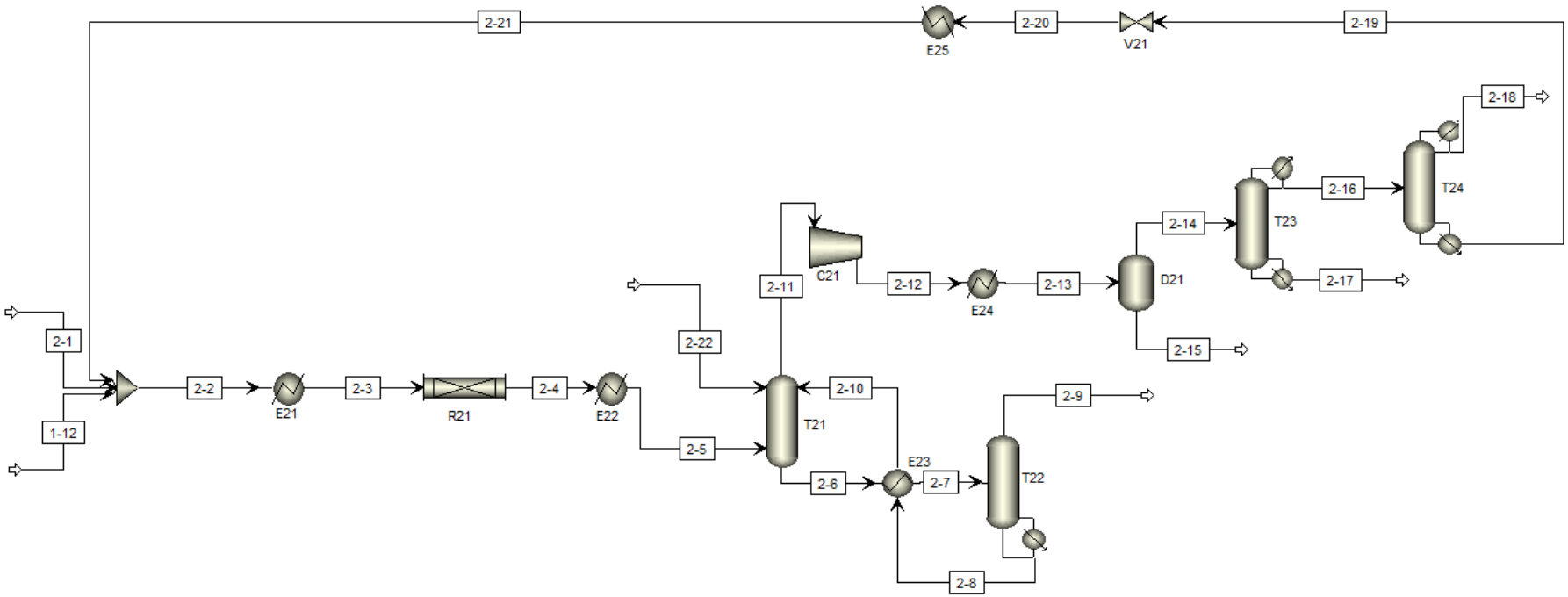

Figure 4.3 OCM process (Section #2).

For ethylene oxide production section, mixed-C2 from OCM process was mixed with oxygen (stream 3-2). Then, gas mixture was compressed and heated to 2.1 MPa and 180°C. The direct oxidation of ethylene to ethylene oxide took place on Ag catalyst packed inside tubular reactor (R-31). Effluent from the reactor including ethylene oxide, carbon dioxide, water and the remaining of ethane and ethylene (stream 3-6) was fed to separate ethylene oxide from the mixture via the physical absorption of water (stream 3-7) at high pressure. The bottom product from absorber which was the mixture of ethylene oxide and water (stream 3-9) was separated by distillation column (T31) while the light gas (stream 3-8) consisting mainly of ethane was collected as a by-product from the process. Ethylene oxide (stream 3-11) was fed to the next section. The scheme for this section was portrayed as in Figure 4.4.

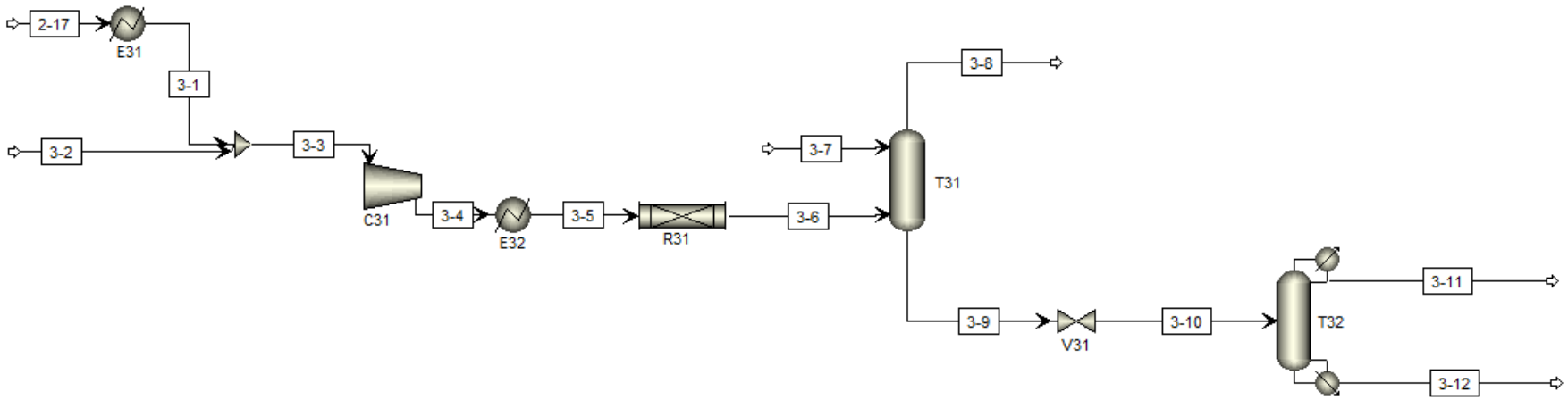

Figure 4.4 EO production (Section #3)

Pressure of ethylene oxide was increased to 2.5 MPa while carbon dioxide from Section #1 (stream 1-7) and Section #2 (stream 2-9) were mixed and followed by removing of water vapor. Pressure of carbon dioxide was increased to 2.5 MPa before mixing with ethylene oxide. Temperature of the mixture was cooled down to 120°C for the condition of the reaction. The carboxylation of ethylene oxide to ethylene carbonate took place on KI catalyst inside the reactor. Effluent from the reactor including ethylene carbonate, ethylene glycol and the remaining of carbon dioxide and ethylene oxide (stream 4-9) was cooled down to 60°C before entering the separation process. Liquid mixture (stream 4-13) was fed to distillation tower for the separation of ethylene glycol and ethylene carbonate while light gas (stream 4-12) which was mainly of carbon dioxide remaining and other effluent gas were purged out of the process. Ethylene carbonate (stream 4-14) produced from the process was at a hundred percent purity while ethylene glycol (stream 4-15), as a by-product, was obtained at 92% purity. Figure 4.5 displayed the diagram for EC production section.

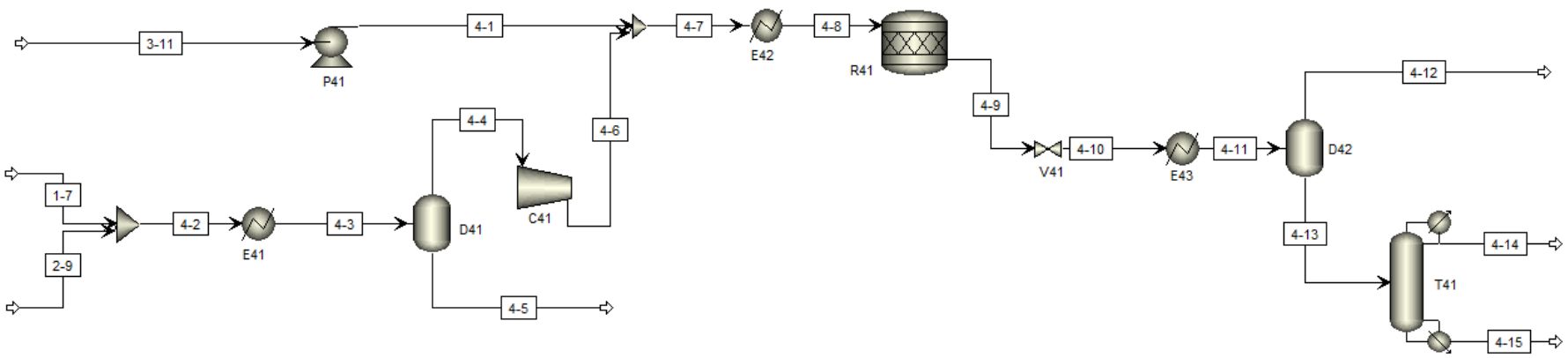

Figure 4.5 EC production (Section #4)

4.2 Process simulation

Each part of the process was simulated in Aspen PLUS®. The following was a detailed process input and specification.

4.2.1 Biogas production and treatment (Section #1)

Input for the biogas production and treatment section including operating condition of main unit operations were summarized in Table 4.1.

Table 4.1 Process input for the biogas production and treatment section

Biogas (stream 1-2)	
Flow rate (kmol/h)	630
Temperature (oC)	30
Pressure (atm)	1
Composition (mol %)	
CH4	42.6
CO2	42.5
H2O	14.9
MEA solution (stream 1-4)	
Flow rate (kmol/h)	4072
Temperature (oC)	30
Pressure (atm)	1
Composition (mol %)	
MEA	70
H2O	30

Absorption column (T11)	
Model	Rate-based with MEA-CO2-H2O kinetic
Number of stages	20
Pressure (atm)	1

Packing	MELLAPAK, Sulzer 250X
Packing height (m)	12
Packing diameter (m)	2
Stripping column (T12)	
Model	Equilibrium
Number of stages	20
Pressure (atm)	1 with 0.02 atm Pdrop
Boilup ratio	0.9
Cooler (E12)	
Outlet temp. (oC)	30

4.2.2 OCM process (Section #2)

Input for the OCM including operating condition of main unit operations were summarized in Table 4.2.

Table 4.2 Process input for the OCM process section

Bio-CH4 (stream 1-12)	
Flow rate (kmol/h)	278
Temperature (oC)	30
Pressure (atm)	1
Composition (mol %)	
CH4	90
CO2	4.2
H2O	5.8
O2 (stream 2-1)	
Flow rate (kmol/h)	144
Temperature (oC)	30
Pressure (atm)	1
Composition (mol %)	
O2	100

MEA solution (stream 2-22)	
Flow rate (kmol/h)	920
Temperature (oC)	30
Pressure (atm)	1
Composition (mol %)	
MEA	70
H2O	30

Packed bed reactor (R21)	
Model	Isothermal tubular reactor with Na-W-Mn/SiO2 kinetic
Resident time (ms)	22.7
Catalyst bed voidage	0.45
Particle density (kg/m3)	1100
Absorption column (T21)	
Model	Rate-based with MEA-CO2-H2O kinetic
Number of stages	20
Pressure (atm)	0.98
Packing	MELLAPAK, Sulzer 250X
Packing height (m)	18
Packing diameter (m)	3
Stripping column (T22)	
Model	Equilibrium
Number of stages	20
Pressure (atm)	1 with 0.02 atm Pdrop
Boilup ratio	0.9
Fired heater (E21)	
Outlet temp. (oC)	850
Cooler (E22)	
Outlet temp. (oC)	30
Cooler (E24)	

Outlet temp. (oC)	30
Cooler (E25)	
Outlet temp. (oC)	30
Deethanizer (T23)	
Model	Shortcut distillation column with partial condenser
Reflux ratio	1.5Rmin
Pressure (atm)	15 atm
CH4 (LK) recovery	99.99%
C2H4 (HK) recovery	0.01%
Demethanizer (T24)	
Model	Shortcut distillation column with partial condenser
Reflux ratio	1.5Rmin
Pressure (atm)	20 atm
O2 (LK) recovery	99.99%
CH4 (HK) recovery	0.01%
Gas compressor (C21)	
Discharge pressure (atm)	10

4.2.3 EO production (Section #3)

Input for the EO production including operating condition of main unit operations were summarized in Table 4.3.

Table 4.3 Process input for the EO production section

C2 from OCM (stream 2-17)	
Flow rate (kmol/h)	111
Temperature (oC)	-27
Pressure (atm)	15
Composition (mol %)	
C2H4	43.6
C2H6	51.4

H2O	5.0
O2 (stream 3-2)	
Flow rate (kmol/h)	44
Temperature (oC)	30
Pressure (atm)	1
Composition (mol %)	
O2	100
H2O absorbent (stream 3-7)	
Flow rate (kmol/h)	350
Temperature (oC)	40
Pressure (atm)	20.73
Composition (mol %)	
H2O	100

Packed bed reactor (R31)	
Model	Isothermal multi-tubular reactor with Ag kinetic
No. of tubes	17642
Tube diameter (mm)	31.3
Tube length (m)	7
Catalyst bed voidage	0.011
Particle density (kg/m3)	590
Absorption column (T31)	
Model	Equilibrium
Number of stages	10
Pressure (atm)	20.72
Vaporizer (E31)	
Vapor fraction	1
Cooler (E32)	
Outlet temp. (oC)	180
Distillation column (T32)	

Model	Shortcut distillation column with partial condenser
Reflux ratio	1.5Rmin
Pressure (atm)	10 atm
EO (LK) recovery	99.99%
H2O (HK) recovery	0.01%

4.2.4 EC production (Section #4)

Input for the EC production including operating condition of main unit operations were summarized in Table 4.4.

Table 4.4 Process input for the EC production section

EO (stream 2-17)	
Flow rate (kmol/h)	61
Temperature (oC)	76.7
Pressure (atm)	10
Composition (mol %)	
EO	99.0
CO2	0.5
C2H6	0.3
O2	0.2
CO2 from Biogas (stream 1-7)	
Flow rate (kmol/h)	1775
Temperature (oC)	99.3
Pressure (atm)	1
Composition (mol %)	
CO2	9.3
H2O	89.9
CH4	0.8
CO2 from OCM (stream 2-9)	
Flow rate (kmol/h)	96

Temperature (oC)	92.7
Pressure (atm)	1
Composition (mol %)	
CO2	20.5
H2O	74.9
C2H4	4.1

Isothermal CSTR reactor (R41)	
Model	RStoic
Temperature (oC)	120
Tube diameter (mm)	31.3
Tube length (m)	7
Catalyst bed voidage	0.011
Particle density (kg/m3)	590
Distillation column (T41)	
Model	Shortcut distillation column with partial condenser
Reflux ratio	1.5Rmin
Pressure (atm)	1 atm
EG (LK) recovery	99.99%
EC (HK) recovery	0.01%
Cooler (E41)	
Outlet temp. (oC)	30
Cooler (E42)	
Outlet temp. (oC)	120
Cooler (E42)	
Outlet temp. (oC)	60
Gas compressor (C41)	
Discharge pressure (atm)	24.67

4.3 Process optimization

After the base case model had been simulated successfully, some parameters of the process i.e. flow rate of the oxygen fed as a reactant for OCM process, OCM reaction temperature, flow rate of the oxygen fed as a reactant for EO production and EO reaction temperature were varied in order to produce more C2 and EO product. The parameters were varied in range below:

- Flow rate of the oxygen fed as a reactant for OCM process: 144 – 300 kmol/h
- OCM reaction temperature: 750-875oC
- Flow rate of the oxygen fed as a reactant for EO production: 44 – 200 kmol/h
- OCM reaction temperature: 131-257oC

4.4 Process heat integration

In order to minimize process duty, the optimized model from section 4.3 was performed process heat integration.

CHAPTER V

RESULTS AND DISCUSSION

5.1 Model validation

This section described method used to validate the two kinetic models i.e. OCM kinetic over Na-W-Mn/SiO2 catalyst reported by M. Daneshpayeh et al., 2009 and direct oxidation of ethylene to ethylene oxide over Ag catalyst reported by Gan et al., 2001. The two mentioned model had been validated before being applied in the simulated process.

5.1.1 Validation of OCM kinetic model over Na-W-Mn/SiO2 catalyst

M. Daneshpayeh et al., 2009 reported the reaction network of OCM reactions over Na-W-Mn/SiO2 catalyst. There were nine heterogeneous catalytic reactions and one homogeneous gas phase reaction included in the proposed reaction network. The kinetic expression and kinetic parameters were mentioned in Table 3.4 and equation 3.2 - 3.7 respectively.

The aforementioned equations were validated by simulation in Aspen Plus. Refer to the experimental of M. Daneshpayeh et al., 2009, the simulated process were shown in Figure 5.1.

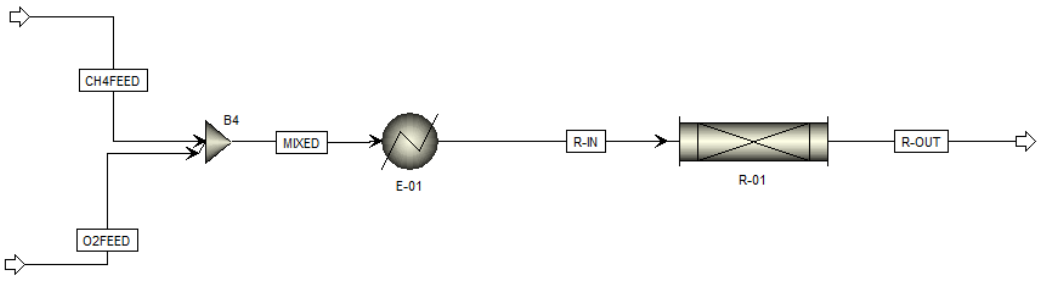

Figure 5.1 Simulated process used in the validation of kinetic model

Each experimental condition i.e. reaction temperature, CH4/O2 ratio and space velocity, were applied in the simulated process in order to calculate CH4 conversion, ethylene selectivity and ethane selectivity. The calculated results obtained from simulation were compared with the results reported in literature. The comparisons were portrayed in Figure 5.2–Figure 5.4.

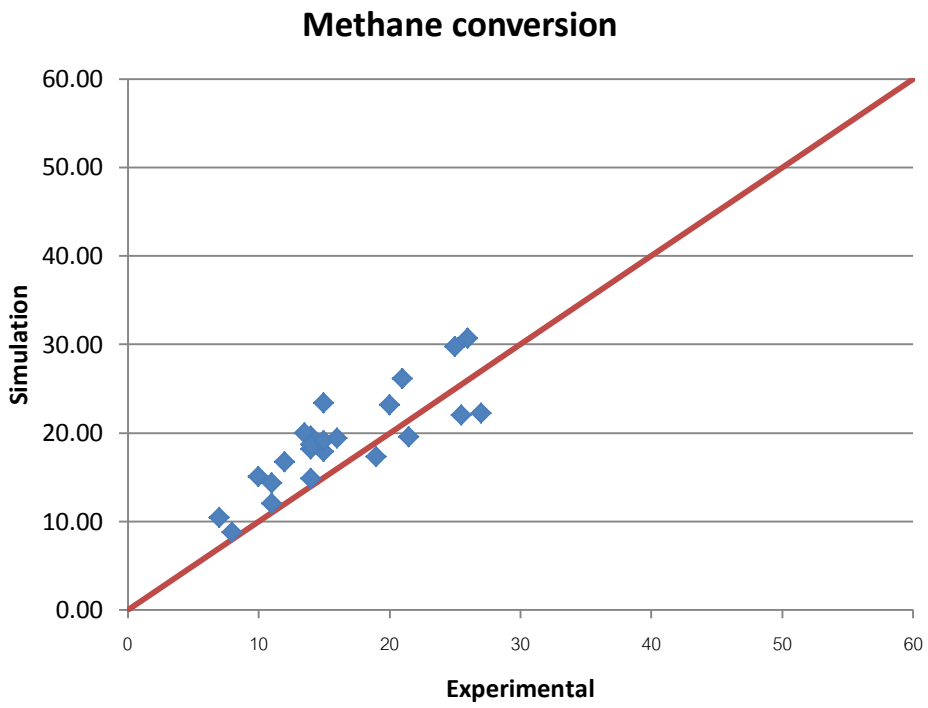

Figure 5.2 Comparison of CH4 conversion

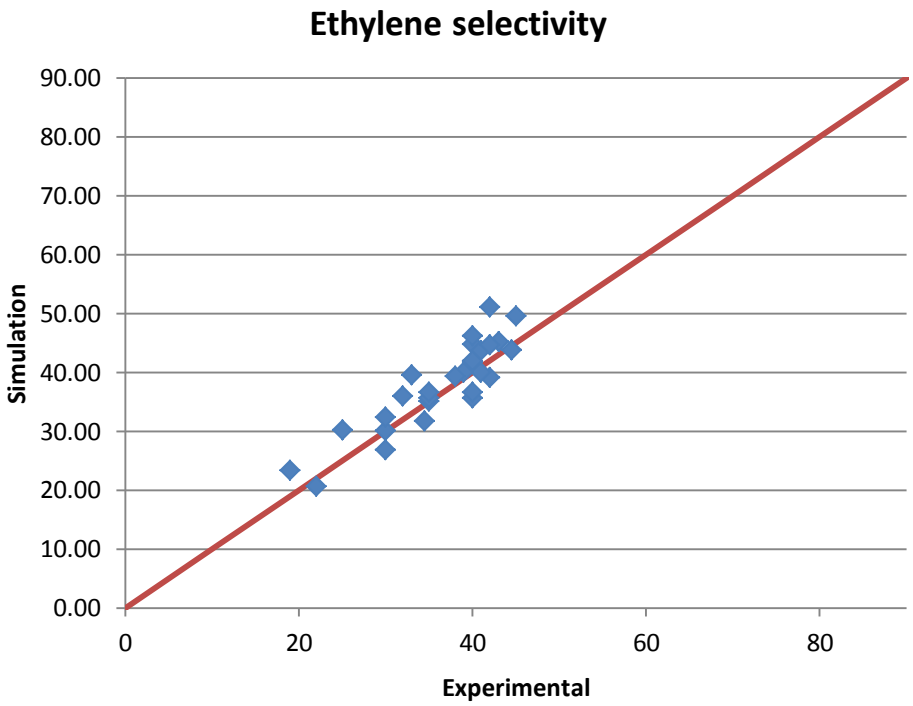

Figure 5.3 Comparison of C2H4 selectivity

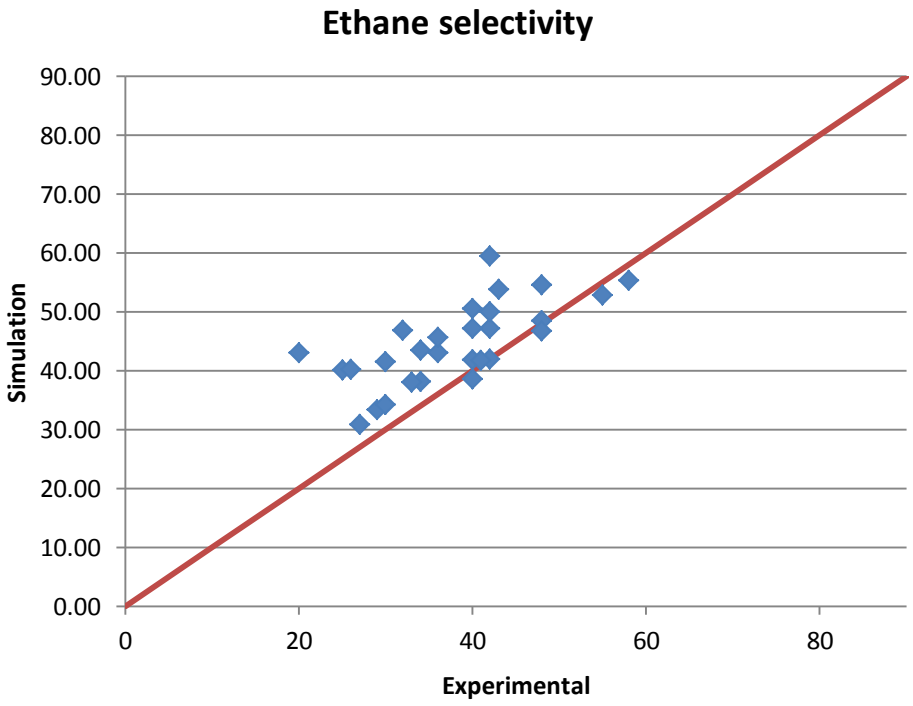

Figure 5.4 Comparison of C2H6 selectivity

From the model validation, the simulated results and the experimental results were in good agreement. Therefore, the kinetic model could be applied in the further simulation.

5.1.2 Validation of EO kinetic model over Ag catalyst

As the same way as OCM kinetic model, the kinetic model of direct oxidation of ethylene to ethylene oxide reported by Gan et al., 2001 were also validated. The aforementioned kinetic model was described by equation 3.14 – 3.19 respectively.

Each experimental condition reported in literature was applied in the simulated process. The calculated results obtained from simulation were compared with the results reported in literature. The comparisons were displayed in Figure 5.5– Figure 5.8.

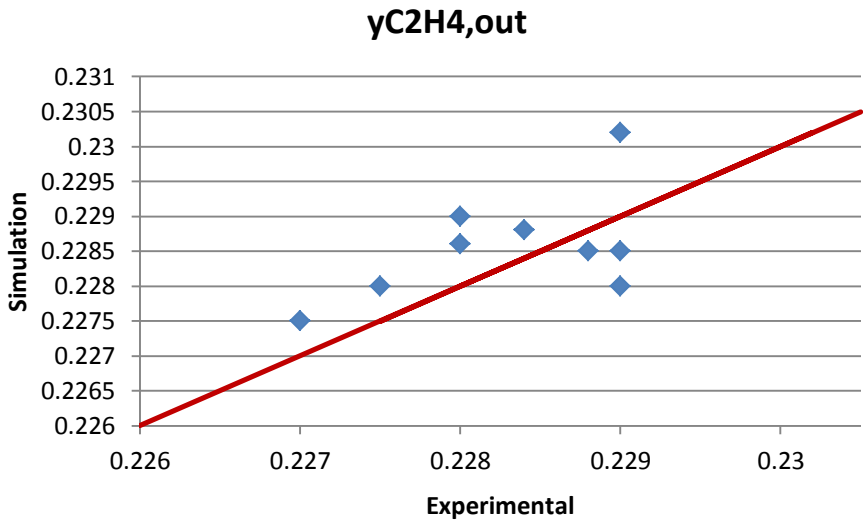

Figure 5.5 Comparison of y_{C2H4} in product stream

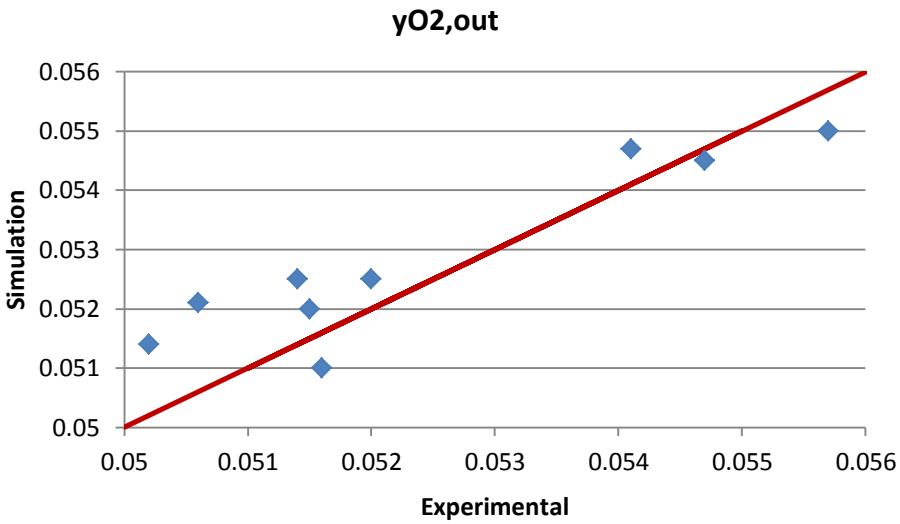

Figure 5.6 Comparison of y_{O2} in product stream

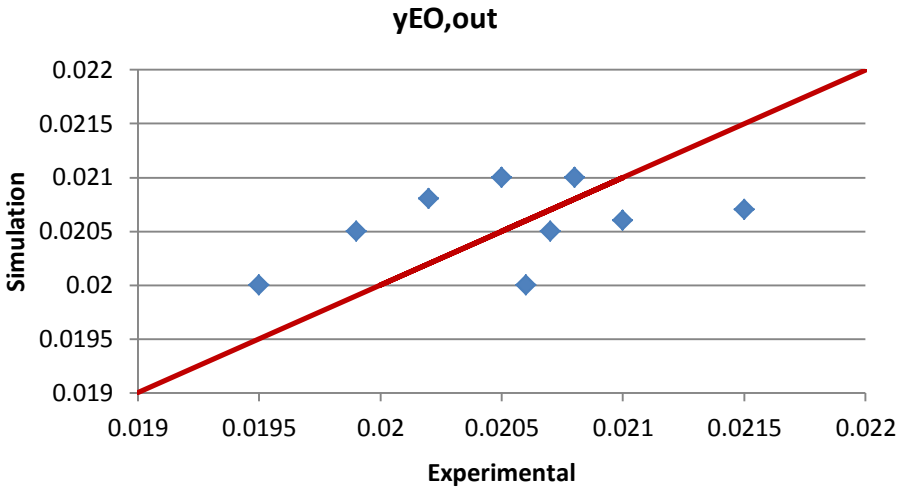

Figure 5.7 Comparison of y_{EO} in product stream

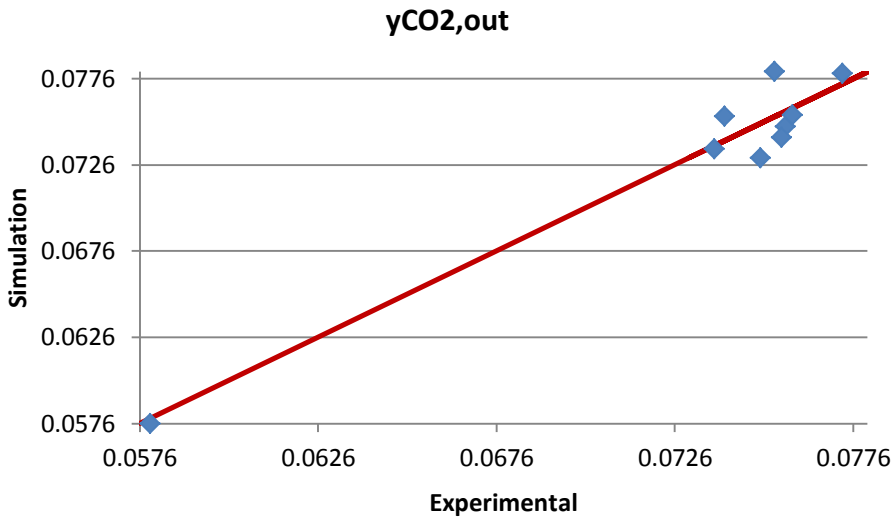

Figure 5.8 Comparison of y_{CO2} in product stream

5.2 Biogas pretreatment results

Results of carbon dioxide treatment by the chemical absorption of MEA solution were shown in Table 5.1 and Table 5.2 respectively.

Table 5.1 Process input-output of biogas pretreatment

	Process input	Process output	
	Biogas (1-2) kmol/h	Bio-CH4 (1-12) kmol/h	CO2 (1-7) kmol/h
H2O	94.14	11.73	1596.58
CO2	268.94	16.03	164.59
CH4	269.29	250.08	14.47
Total	632.36	277.84	1775.64

Table 5.2 Process duty required for biogas pretreatment

Unit operation		Duty req. (kW)
E12	Gas cooler	4256
T12	CO2 Stripper reboiler	23165
	Total	27421

From Table 5.1 and Table 5.2, methane in biogas was recovered by 92.87% with the duty required of 27,421 kW

5.3 OCM-EO-EC Base case model results

In the base case model, the reaction temperature input for the process was at the optimized point reported in the literature i.e. 850oC for the OCM reaction and 180oC for the direct oxidation of ethylene to ethylene oxide reaction. For the amount of oxygen molar flow rate in each process; for OCM, the oxygen was fed at the flow rate that converted completely (no oxygen remaining in each process) i.e. 144 kmol/h; for EO, oxygen was fed at the flow rate of which EO was completely converted i.e. 44 kmol/h respectively.

Table 5.3-Table 5.5 showed the summary of stream results for the base case model of OCM process, EO process and EC process.

Table 5.3 Summary of input-output for OCM base case process

	One-pass		Overall					
	Reactor inlet (2-3) kmol/h	Reactor outlet (2-4) kmol/h	**Process feed** kmol/h	**Process output** Mixed C2 (2-17)	Purge (2-18)	Water (2-15)	CO2 (2-9)	**Total kmol/h**
H2		0.72			0.72			0.72
CO		7.97			7.97			7.97
O2	144.00	0.01	144.00		0.01			0.01
CH4	1316.48	1066.49	250.06	0.11	0.11		0.01	0.23
C2H4		50.58		48.47			0.86	49.33
C2H6		57.12		57.12				57.12
CO2	16.12	42.74	16.12				11.04	11.04
H2O	11.67	238.42	11.67	5.43		101.99	55.02	162.44

Table 5.4 Summary of input-output for EO base case process

	One-pass		Overall				
	Reactor inlet (3-5) kmol/h	Reactor outlet (3-6) kmol/h	**Process feed** kmol/h	**Process output**			
				EO (3-11)	Fuel (3-8)	Water (3-12)	**Total kmol/h**
H2							
CO							
O2	44.00	10.64	44.00	0.02	10.62		10.64
CH4	0.11	0.11	0.11		0.11		0.11
C2H4	48.47	1.80	48.47	0.01	1.79		1.80
C2H6	57.12	57.12	57.12	0.20	56.91		57.12
CO2		8.02		0.14	7.88		8.02
EO		42.66		42.64	0.02		42.66
H2O	5.43	13.46	5.43	0.04	0.37	363.06	363.46

Table 5.5 Summary of input-output for EC base case process

	One-pass		Overall								
			Process feed				Process output				
	Reactor inlet (4-7) kmol/h	Reactor outlet (4-8) kmol/h	EO (3-11)	CO2-biogas (1-7)	CO2-OCM (2-9)	**Total kmol/h**	EC (4-15)	EG (4-14)	CO2-Off (4-12)	Water (4-5)	**Total kmol/h**
H2											
CO											
O2	0.02	0.02	0.02		0.00	0.02			0.02		0.02
CH4	14.48	14.48		14.47	0.01	14.48		0.00	14.48		14.48
C2H4	0.87	0.87	0.01		0.86	0.86		0.00	0.86		0.87
C2H6	0.20	0.20	0.20		0.00	0.20			0.20		0.20
CO2	175.66	139.84	0.14	164.59	11.04	175.78		0.32	139.52	0.12	139.84
EO	42.64	0.43	42.64			42.64		0.04	0.38		0.43
H2O	8.53	2.14	0.04	1596.58	55.02	1651.63		1.63	0.51	1643.10	2.14
EG		6.40						6.37	0.024		6.40
EC		35.81					35.78		0.03		35.81

From Table 5.3, methane was 18.99% one-pass converted, resulting in 3.84% of ethylene yield and 4.33% ethane yield respectively. However, for overall process calculation, methane was 99.91% converted, ethylene and ethane yield was shifted up to 19.73% of ethylene and 22.84% of ethane respectively.

From Table 5.4, because EO process did not have a recycle stream, therefore, one-pass calculation resulted as the same as overall calculation. The process converted 96.29% of ethylene which resulted in 65.41% yield of ethylene oxide, 12.3% yield of CO2 and H2O.

From Table 5.5, because EC process did not have a recycle stream, therefore, one-pass calculation resulted as the same as overall calculation. The process converted 99% of ethylene oxide which resulted in 84% yield of ethylene carbonate, 15% yield of ethylene glycol. Moreover, the amount of CO2 consumed by the EC production process was 35.81 kmol/h or 20.39% of carbon dioxide conversion.

5.4 Effect of process key parameters

In order to find the optimum point of operation for each process, there were four parameters that were varied; oxygen feed for OCM process, OCM reaction temperature, oxygen feed for EO process and EO reaction temperature, to find out the effect of these parameters on production of C2, ethylene oxide and CO2 consumption.

5.4.1 Oxygen feed flow rate for OCM process

Oxygen feed flow rate for OCM process was varied between 144 – 300 kmol/h while flow rate of each component in OCM process were monitored. The results was shown in Figure 5.9.

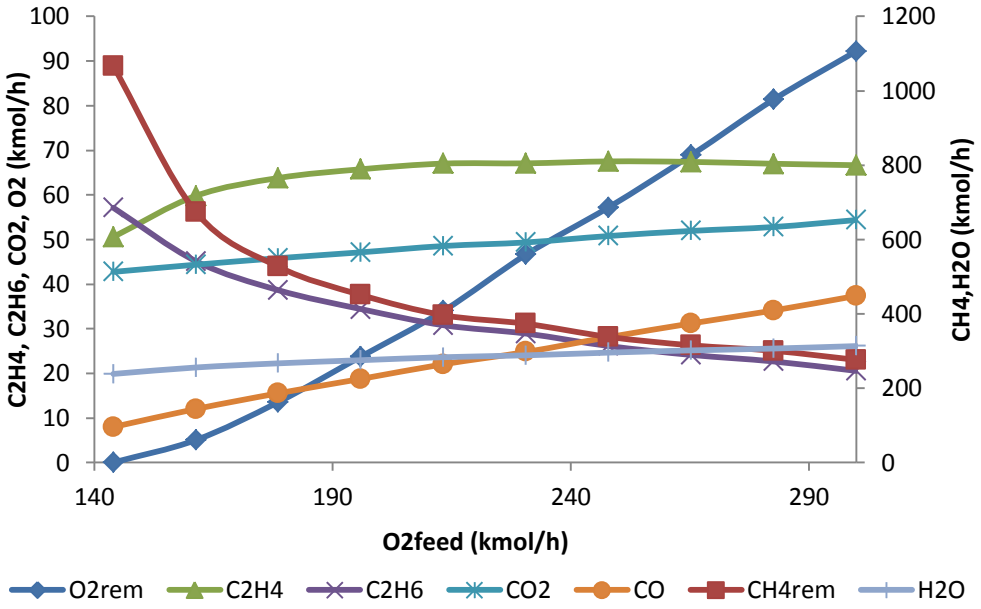

Figure 5.9 Effect of O2 feed flow rate on productivity of OCM process

From Figure 5.9, while more oxygen was fed into the process, more methane was consumed. Moreover, productivity of ethylene was increased but the productivity of ethane was decreased. That showed the increase of ethylene selectivity. However, increase the oxygen feed more than 230 kmol/h was not resulting in the increase of ethylene productivity anymore. At more than 230 kmol/h of oxygen feed, the reaction network tended to favor to produce more carbon dioxide, carbon monoxide and water, which referred to the combustion of methane. Thus, the optimum point of oxygen feed flow rate was 230 kmol/h respectively.

5.4.2 OCM reaction temperature

At oxygen feed flow rate of 230 kmol/h, the temperature of OCM reactor was varied between 750 – 950oC while flow rate of each component in OCM process were monitored. The results were shown in Figure 5.10.

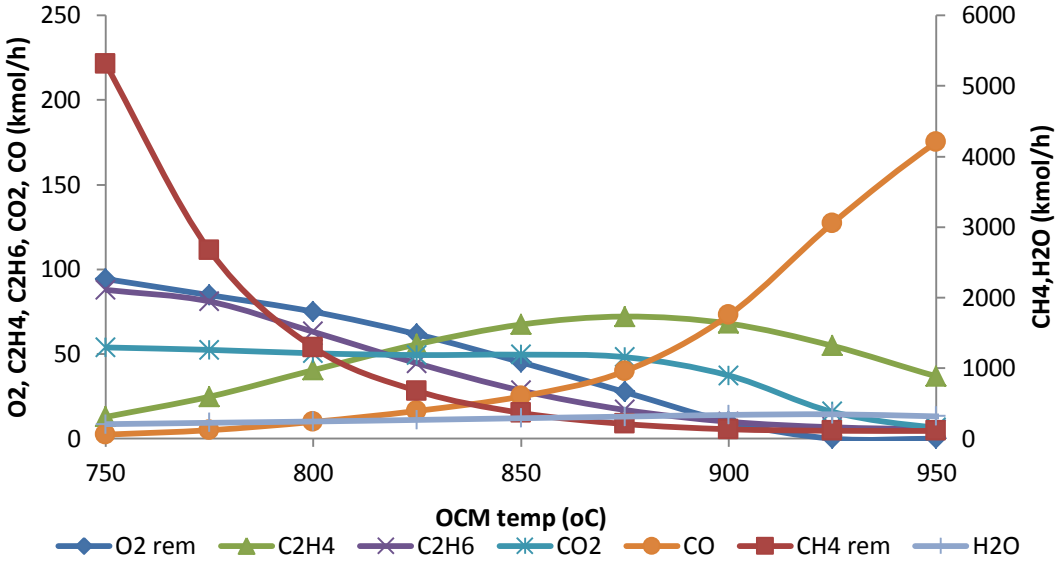

Figure 5.10 Effect of OCM reaction temperature on productivity of OCM process

As seen in Figure 5.10, increasing of OCM reaction temperature resulted in increase of ethylene productivity and decrease of ethane productivity. That referred to the increase of ethylene selectivity. However, rising temperature to more than 875oC resulted in the decrease of ethylene productivity and increase of carbon monoxide productivity instead. It was due to the amount of oxygen feed which was the limiting reactant for this process. Nevertheless, this reaction kinetic reported by M. Daneshpayeh et al., 2009 was valid in the temperature range of 750 – 875oC respectively. Therefore, the optimum point of OCM reaction temperature was at 875oC.

5.4.3 Oxygen feed flow rate for EO production

In case of EO process, oxygen feed flow rate for EO process was varied between 44 – 120 kmol/h while flow rate of each component in EO process were monitored. The results were shown in Figure 5.11.

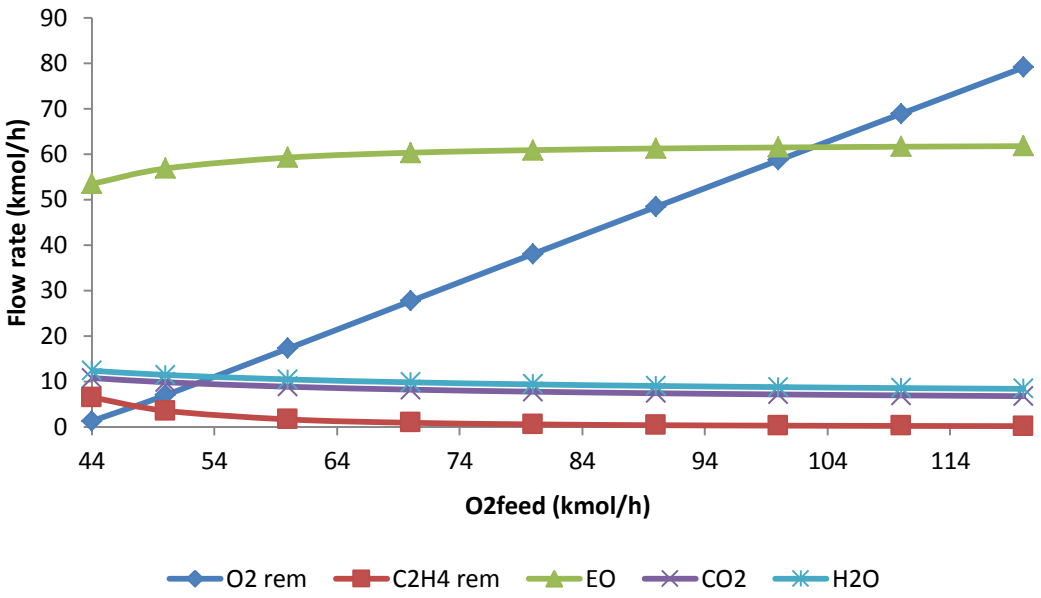

Figure 5.11 Effect of O2 feed flow rate on productivity of EO process

From Figure 5.11, increase of oxygen feed flow rate resulted in increase of ethylene oxide productivity. However, it was due to the amount of ethylene which was a limiting reactant, therefore, increasing of oxygen feed flow rate more than 60 kmol/h was unnecessary. Thus, the optimum point of oxygen flow rate for EO production was 60 kmol/h.

5.4.4 EO reaction temperature

At oxygen feed flow rate of 60 kmol/h, the temperature of DoE reactor was varied between 131.85 – 256.85oC while flow rate of each component in OCM process were monitored. The results was shown in Figure 5.12.

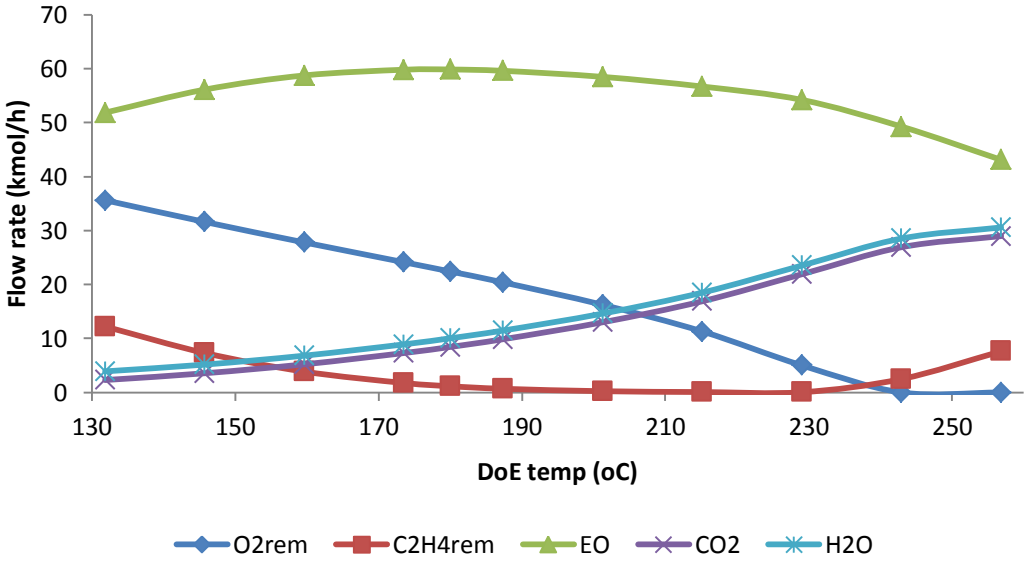

Figure 5.12 Effect of DoE reaction temperature on productivity of EO process

As seen in Figure 5.12, increase of DoE reaction temperature resulted in increase of ethylene oxide productivity. However, productivity of ethylene oxide was dropped when the temperature was increased to more than 180oC. It was due to the limiting amount of ethylene reactant. At higher temperature, when ethylene was completely consumed while oxygen was remaining, there was a chance that oxygen would react with ethylene oxide resulting in the formation of carbon dioxide and water. Moreover, at temperature more than 240oC, this was the point that oxygen was completely consumed, there were increase of ethylene productivity while ethylene oxide continue decreasing, it could be implied that ethylene oxide was converted backward into ethylene. Thus, the optimum point of DoE reaction temperature was at 180oC respectively.

5.5 Optimized model results

After the optimum conditions for each process were applied, the optimized model results were showed in Table 5.6-Table 5.8.

Table 5.6 Summary of input-output for OCM optimized process

	One-pass		Overall					
	Reactor inlet (2-3) kmol/h	Reactor outlet (2-4) kmol/h	Process feed kmol/h	Process output				
				Mixed C2 (2-17)	Purge (2-18)	Water (2-15)	CO2 (2-9)	Total kmol/h
H2		3.87			3.87			3.87
CO		39.56			39.55			39.55
O2	230.00	28.10	230.00		28.10			28.10
CH4	460.43	210.40	250.06	0.02	0.02		0.01	0.05
C2H4		72.11		65.22			3.47	68.69
C2H6		17.17		17.17				17.17
CO2	16.12	48.01	16.12				17.77	17.77
H2O	11.67	312.11	11.67	1.61		61.49	54.65	117.75

Table 5.7 Summary of input-output for EO optimized process

	One-pass		Overall				
	Reactor inlet (3-5) kmol/h	Reactor outlet (3-6) kmol/h	Process feed kmol/h	Process output			
				EO (3-11)	Fuel (3-8)	Water (3-12)	Total kmol/h
H2							
CO							
O2	65.00	22.42	65.00	0.08	22.34		22.42
CH4	0.02	0.02	0.02		0.02		0.02
C2H4	65.22	1.15	65.22	0.01	1.14		1.15
C2H6	17.17	17.17	17.17	0.15	17.03		17.17
CO2		8.44		0.31	8.13		8.44
EO		59.85		59.84		0.01	59.85
H2O	1.61	10.05	1.61	0.04	0.22	359.79	10.05

Table 5.8 Summary of input-output for EC optimized process

	One-pass		Overall								
			Process feed				Process output				
	Reactor inlet (4-7) kmol/h	Reactor outlet (4-8) kmol/h	EO (3-11)	CO2-biogas (1-7)	CO2-OCM (2-9)	**Total kmol/h**	EC (4-15)	EG (4-14)	CO2-Off (4-12)	Water (4-5)	**Total kmol/h**
H2											
CO											
O2	0.08	0.08	0.08			0.08			0.08		0.08
CH4	14.48	14.48		14.47	0.01	14.47			14.47		14.48
C2H4	3.48	3.48	0.01		3.47	3.48		0.01	3.47		3.48
C2H6	0.15	0.15	0.15			0.15			0.15		0.15
CO2	182.55	132.29	0.31	164.59	17.77	132.29		0.45	131.84	0.12	132.41
EO	59.84	0.63	59.84			0.63		0.09	0.54		0.63
H2O	8.95		0.04	1596.58	54.65					1642.32	1642.32
EG		8.946					0.001	8.921	0.024		8.946
EC		50.267					50.228	0.005	0.033		50.266

From Table 5.6, methane was 54.3% one-pass converted, resulting in 15.66% of ethylene yield and 3.73% ethane yield respectively. However, for overall process calculation, methane was 99.98% converted, ethylene and ethane yield was shifted up to 27.47% of ethylene and 6.87% of ethane respectively.

From Table 5.7, because EO process did not have a recycle stream, therefore, one-pass calculation resulted as the same as overall calculation. The process converted 98.23% of ethylene which resulted in 91.76% yield of ethylene oxide, 12.94% yield of CO2 and H2O.

From Table 5.8, because EC process did not have a recycle stream, therefore, one-pass calculation resulted as the same as overall calculation. The process converted 98.95% of ethylene oxide which resulted in 84% yield of ethylene carbonate, 14.95% yield of ethylene glycol. Moreover, the amount of CO2 consumed by the EC production process was 50.27 kmol/h or 27.54% of carbon dioxide conversion.

5.6 Process heat integration

After the optimized model was obtained, it was performed heat-integration in OCM process. Instead of supplying utility directly into unit operation, each of process equipment was supplied energy from process stream. The heat integrate diagram was shown in Figure 5.13.

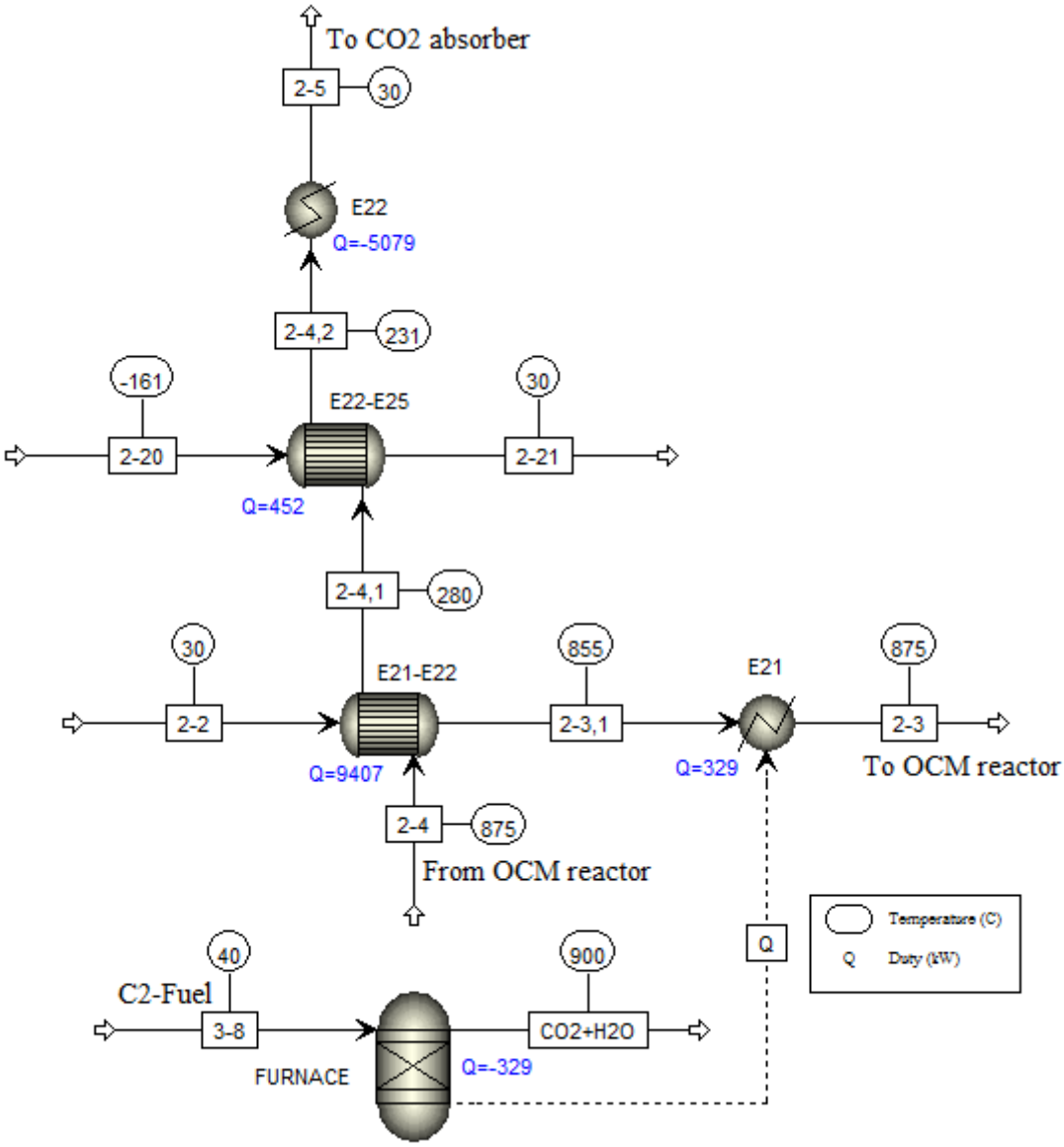

Figure 5.13 Heat-integrated diagram for OCM process

From Figure 5.13, the mixed feed stream (stream 2-2) was heated to 850oC by the effluent stream from OCM reactor (stream 2-4). However, stream 2-3,1 required more energy to reach 875oC which was a reaction temperature, the energy was obtained by heat of combustion from C2-Fuel (stream 3-8) at 900oC. The OCM effluent (stream 2-4,1) was able to heat the methane recycle stream (stream 2-20) to reach 30oC. Moreover, before entering CO2 absorber column, stream 2-4,2 remained energy about 5,000 kW to use as a utility for the process. The detailed process duty was shown in Table 5.9 respectively.

Table 5.9 Process duty for base case, optimized case and heat-integrated case.

Unit operation	Base case (kW)	Optimized (kW)	Heat-int. (kW)
Major heat exchanger			
E21 Feed preheater	19644	9713	329
E22 Effluent cooler	21070	12287	5079
E24 Wet-gas cooler	5378	2177	2177
E25 Recycled-gas heater	3341.97	779.167	0
Total (kW)	**49434**	**24956**	**7585**
Minor heat exchanger			
R21 Reactor	14617	18955	18955
T22 Stripper reboiler	1201	1334	1334
T23 De-C1 condensor	820	412	412
T23 De-C1 reboiler	1309	397	397
T24 De-C2 condensor	4181	1012	1012
T24 De-C2 reboiler	2541	620	620
Total (kW)	**74103**	**47686**	**30315**
Productivity (kmol C2H4/h)	**48.47**	**65.22**	**65.22**
Total (kW/kmol C2H4/h)	**1528.97**	**731.16**	**464.81**

As seen in Table 5.9, in optimized model, feed preheater (E21) required energy of 9,713 kW to heat the mixed feed stream to 875oC, which resulted in about 141 kmol/h (6211 kg/h) of carbon dioxide from the combustion of 325 kmol/h of C2-Fuel. That was large amount of carbon dioxide released to the atmosphere. However, the heat-integrated model solved that problem. It required only 329 kW of energy to heat the mixed feed to 875oC. That resulted in only 5 kmol/h of carbon dioxide generated from the combustion of 11 kmol/h of C2-Fuel respectively.

In case of the duty required per unit of C2H4 productivity, the base case model required energy of 1,523 kW per kmol/h of C2H4 while the optimized model

required 731 kW per kmol/h of C2H4 and the heat-integrated model required only 465 kW per kmol/h. Thus, the heat-integrated model showed a great performance that could be challenged with the conventional process of C2 production interestingly.

CHAPTER VI

CONCLUSION

6.1 Conclusion

Design and development of ethylene carbonate production process from biomass was studied in this research. First of all, bio-methane was produced from wheat straw by the anaerobic digestion process followed by the CO2 absorption by MEA solution. Bio-methane was then brought to produce C2 products via the oxidative coupling of methane (OCM) on Na-W-Mn/SiO2 catalyst. Then, ethylene was fed to produce ethylene oxide via the direct oxidation of ethylene (DoE). Finally, ethylene oxide together with carbon dioxide from biogas treatment section and by-product of OCM section were reacted to form an ethylene carbonate.

Process model was successfully simulated by Aspen Plus® program. In case of OCM reaction network, a rigorous kinetic model expression including nine heterogeneous catalytic reaction and one homogeneous gas phase reaction were employed. For ethylene oxide production, the kinetic model of direct oxidation of ethylene over a conventional Ag catalyst was also employed. For ethylene carbonate production, the experimental data of product distribution, yields and selectivity reported in literature was brought to apply in the process. Once the base case model had been developed, process key parameters i.e. oxygen feed flow rate for OCM process, OCM reaction temperature, oxygen feed flow rate for EC process and EO reaction temperature were varied to find the optimum point of operating conditions that yielded more ethylene productivity, ethylene oxide productivity and carbon dioxide consumption, respectively. Finally, the optimized model had been performed the heat integration method to minimize the energy consumption of the process.

For biogas production and treatment, 200,000 tons per year of wheat straw yielded 630 kilomoles per hour (17,850 kilograms per hour) of biogas, which was treated and yielded 278 kilomoles per hour of bio-methane. CO2 treatment process for biogas required process duty of 27,421 kW.

As a result in base case model, OCM process was operated at 144 kmol/h of oxygen feed flow rate and reaction temperature of 850oC. EO process was operated at 44 kmol/h and reaction temperature of 180oC. At the mentioned operating condition, oxygen as the limiting reactant of each process was completely consumed. The OCM process converted 99.91% of methane and yielded 19.73% of ethylene and 22.84% of ethane respectively. EO process consecutively converted 96.29% of ethylene and yielded 65.41% of ethylene oxide and 12.3% of carbon dioxide and water. Finally, EC production process converted 99% of ethylene oxide and yielded 84% of ethylene carbonate. Carbon dioxide from biogas treatment section and OCM section were 20.39% consumed.

As results of process key parameters study, for OCM process, increasing in oxygen feed flow rate led to the increase of methane one-pass conversion. More methane was converted selectively to ethylene. Anyway, increase oxygen flow rate more than 230 kmol/h resulted in the favor of reaction network to produce more carbon dioxide and carbon monoxide. Thus, the optimum amount of oxygen feed flow rate was 230 kmol/h. For OCM reaction temperature, increasing temperature resulted in the increase of methane one-pass conversion. More methane was converted selectively to ethylene. However, rising temperature to more than 875oC showed the favor of combustion of methane reaction into carbon dioxide and carbon monoxide. Therefore, the optimum reaction temperature was 875oC. For EO process, increasing in oxygen feed flow rate led to the increase of ethylene oxide productivity. The optimum point for oxygen flow rate was at 60 kmol/h, which showed the complete ethylene consumption. For DoE reaction, increase of DoE reaction temperature resulted in increase of ethylene oxide productivity. The

optimum point for DoE reaction temperature was at 180oC in which ethylene was completely consumed.

As a result in optimized model, OCM process was operated at 230 kmol/h of oxygen feed flow rate and reaction temperature of 875oC. EO process was operated at 60 kmol/h and reaction temperature of 180oC. The OCM process converted 99.98% of methane and yielded 27.47% of ethylene and 6.87% of ethane respectively. EO process consecutively converted 98.23% of ethylene and yielded 91.76% of ethylene oxide and 12.94% of carbon dioxide and water. Finally, EC production process converted 98.95% of ethylene oxide and yielded 84% of ethylene carbonate. Carbon dioxide from biogas treatment section and OCM section was 27.54% consumed.

To summarize, for an optimized model, the overall process could convert 100 tons per year of wheat straw ($5,477 per year, Manitoba Agriculture, Food and Rural Development, Canada, 2014) to about 20.57 tons per year of ethylene carbonate (about $1,800/ton, Linyi Lixin Chemicals, China). Thus, this process could make profit of $31,282 per 100 tons of wheat straw respectively. Note that the calculated profit did not include the utility cost and operating cost.

In order to minimize energy consumption of the process, the optimized model was brought to perform process heat integration. In comparison, the base case model required energy of 1,523 kW per kmol/h of C2H4 while the optimized model required 731 kW per kmol/h of C2H4 and the heat-integrated model required only 465 kW per kmol/h respectively. Furthermore, the heat-integrated model dramatically reduced the amount of fuel consumption for furnace preheater (E21) of OCM process from 325 kmol/h to 11 kmol/h of C2 fuel, which resulted in the decrease of carbon dioxide releasing into the atmosphere.

This study provided a green chemical production concept, which started from using biomass as raw materials instead of petroleum to produce C2. OCM reaction was a novel method to produce C2 hydrocarbons alternatively from the conventional catalytic cracking process. Furthermore, about thirty percent of carbon dioxide generated from other parts of the process was utilized by reacting with ethylene oxide to form an ethylene carbonate. However, for OCM process, yields of C2 were still limited to about 30% due to the catalyst activity which resulted in requirement of high process duty. Therefore, to increase the challenges of this process, more effective catalyst should be developed in order to increase more C2 productivity and selectivity so as to utilize more carbon dioxide from the process effectively.

REFERENCES

Alcaide, F., Cabot, P.L., and Brillas, E. "Review Fuel cells for chemicals and energy cogeneration," *Journal of Power Sources*, 153, 47–60 (2006)

Au, C.T., He, H., Lai, S.Y., and Ng, C.F. "The oxidative coupling of methane over $BaCO_3$/LaOC1 catalysts," *Applied Catalysis*, 159, 133-145 (1997)

Au, C.T., Zhou, X. P., Liu, Y. W., Ji, W. J. and Ng, C. F. "The Characterization of BaF_2/Y_2O_3 Catalysts for the OCM Reaction," *Journal of catalysis*, 174, 153–163 (1998)

Buysch H.J., AG B., "Carbonic Ester", Ullmann's Encyclopedia of Industrial Chemistry, 1-18

Chao, Z.S., Zhou, X.P., Wan, H.L., and Tsai, K.R. "Methane oxidative coupling on BaF_2/LaOF catalyst," *Applied Catalysis*, 130, 127-133 (1995)

Chua, Y.T., Mohamed, A.R., and Bhatia, S. "Oxidative coupling of methane for the production of ethylene over sodium-tungsten-manganese-supported-silica catalyst (Na-W-Mn/SiO_2)," *Applied Catalysis*, 343, 142–148 (2008)

Daneshpayeh M., Khodadadi A., Mostoufi N., Mortazavi Y., "Kinetic modeling of oxidative coupling of methane over Mn/Na2WO4/SiO2catalyst", *Fuel Processing Technology*, 90, 403–410 (2009)

Dedov, A.G., Loktev, A.S., Moiseev, I.I., Aboukais, A., Lamonier, J.-F. and Filimonov, I.N. "Oxidative coupling of methane catalyzed by rare earth oxides Unexpected synergistic effect of the oxide mixtures," *Applied Catalysis*, 245, 209–220 (2003)

Fakhroueian, Z., Farzaneh, F., and Afrookhteh, N. "Oxidative coupling of methane catalyzed by Li, Na and Mg doped $BaSrTiO_3$," *Fuel*, 87, 2512–2516 (2008)

Gan, L., Wang, H., Bingchen, Z., Maosheng, X., "Global kinetics and deactivation of Ag-catalyst for ethylene oxide synthesis", *Journal of Chemical Industry and Engineering (China),* 52 (11), 969–972 (2001)

Gao, Z., and Ma, Y. "Direct oxidation of methyl radicals in OCM process deduced from correlation of product selectivities," *Journal of Natural Gas Chemistry*, 19, 534–538 (2010)

Gao, Z., and Shi, Y. "Suppressed formation of CO_2 and H2O in the oxidative coupling of methane over La_2O_3/MgO catalyst by surface modification," *Journal of Natural Gas Chemistry*, 19, 173–178 (2010)

Growing Opportunities, "Guidelines for estimating wheat straw biomass production costs 2014", Manitoba Agriculture, Food and Rural Development (MAFRD), Canada, 2014

Haag, S., Veen, A.C.V., and Mirodatos, C. "Influence of oxygen supply rates on performances of catalytic membrane reactors Application to the oxidative coupling of methane," *Catalysis Today*, 127, 157–164 (2007)

Hong, J.H., and Yoon, K.J. "Oxidative coupling of methane over calcium chloride-promoted calcium chlorophosphate," *Applied Catalysis*, 205, 253–262 (2001)

Hugill, J.A., Tillemans, F.W.A., Dijkstra, J.W., and Spoelstra, S. "Feasibility study on the co-generation of ethylene and electricity through oxidative coupling of methane," *Applied Thermal Engineering*, 25, 1259–1271 (2005)

Ji, S., et al., "Surface WO_4 tetrahedron: the essence of the oxidative coupling of methane over M–W–Mn/SiO_2 catalysts," *Journal of Catalysis*, 220, 47–56 (2003)

Ji, S., et al., "The relationship between the structure and the performance of Na-W-Mn/SiO_2 catalysts for the oxidative coupling of methane," *Applied Catalysis*, 225, 271-284 (2002)

Jiang, Y., Yu, C., Li, W., Yan, J., and Ji, Y. "A reaction-separation combined OCM process for high C_2 hydrocarbon yields, Natural Gas Conversion IV," *Studies in Surface Science and Catalysis*, 107, (1997)

KELLER, G.E., and BHASIN, M. M. "Synthesis of Ethylene via Oxidative Coupling of Methane," *Journal of Catalysis*, 73, 9-19. (1982)

Khodadadian, M., Taghizadeh, M., and Hamidzadeh, M. "Effects of various barium precursors and promoters on catalytic activity of Ba–Ti perovskite catalysts for oxidative coupling of methane," *Fuel Processing Technology*, (2010)

Kiatkittipong, W., Tagawab, T., Goto, S., Assabumrungrata, S., and Praserthdama, P. "TPD study in LSM/YSZ/LaAlO system for the use of fuel cell type reactor," *Solid State Ionics*, 166, 127–136 (2004)

Kirk-Othmer Encyclopedia of Chemical Technology, 4th Edition, 450-466

Kothandraman A., "Carbon Dioxide Capture byChemical Absorption: A Solvent Comparison Study", Ph.D. Thesis, Massachusetts Institute of Technology, 2010

Lee M. R., Park M.J., Jeon W., Choi J.W., Suh Y.W., Suh D.J., "A kinetic model for the oxidative coupling of methane over Na2WO4/Mn/SiO2", *Fuel Processing Technology*, 96, 175–182 (2012)

Li, H., and Wang, J. "Study onCO2 reforming of methane to syngas overAl2O3–ZrO2 supported Ni catalysts prepared via a direct sol–gel process," *Chemical Engineering Science*, 59, 4861–4867 (2004)

Lim Y., Kim J., Jung J., Lee C.S., Han C., "Modeling and Simulation of CO2Capture Process for Coal-based Power Plant using Amine Solvent in South Korea", *Energy Procedia*, 37, 1855 – 1862 (2013)

Lin, Y. S., and Zeng, Y. "Catalytic Properties of Oxygen Semipermeable Perovskite-Type Ceramic Membrane Materials for Oxidative Coupling of Methane," *Journal of catalysis*, 164, 220–231 (1996)

Liu, H., Wang, X., Yang, D., Gao, R., Wang, Z., and Yang, J. "Scale up and stability test for oxidative coupling of methane over Na_2WO_4-Mn/SiO_2 catalyst in a 200 ml fixed-bed reactor," *Journal of Natural Gas Chemistry*, 17, 59–63 (2008)

Liu, S., Tan, X., Li, K., and Hughes, R. "Methane coupling using catalytic membrane reactors," *Catalysis review*, 43:1, 147-198 (2001)

Long, R.Q., Zhou, S.Q., Huang, Y.P., Weng, W.Z., Wan, H.L., and Tsai, K.R. "Promoting effect of F- on Sr/La oxide catalysts for the oxidative coupling of methane," *Applied Catalysis*, 133, 269-280 (1995)

Mahmoodi, S., Ehsani, M.R., and Ghoreishi, S.M. "Effect of promoter in the oxidative coupling of methane over synthesized Mn/SiO_2 nanocatalysts via incipient wetness impregnation," *Journal of Industrial and Engineering Chemistry*, 16, 923–928 (2010)

Moioli S., Pellergrini A., Gamba S., “Simulation of CO2capture by MEA scrubbing with a rate-based model”, *Procedia Engineering*, 42, 1651 – 1661 (2012)

Murata, K., Hayakawa, T., Hamakawa, S., and Suzuki, K. “Lithium-doped sulfated-zirconia catalysts for oxidative coupling of methane to give ethylene and ethane,” *Catalysis Today*, 45, 41-45 (1998)

Naskar S., Jana K., De S., “COMPARATIVE PERFORMANCE STUDY OF CO2 CAPTURE WITH MONOETHYL AND DIETHYL AMINES USING ASPEN PLUS®”, *International Journal of Emerging Technology and Advanced Engineering*, 3 (3), 490-497 (2013)

Oexmann J., Kather A., “Post-combustion CO2capture in coal-fired power plants: comparison of integrated chemical absorption processes with piperazine promoted potassium carbonate and MEA”, *Energy Procedia*, 1, 799-806 (2009)

Oi L.E., “Comparison of Aspen HYSYS and Aspen Plus simulation of CO2 absorption into MEA from atmospheric gas”, *Energy Procedia*, 23, 360 – 369 (2012)

Papa, F., Gingasu, D., Patron, L., Miyazaki, A., and Balint, I. “On the nature of active sites and catalytic activity for OCM reaction of alkaline-earth oxides-neodymia catalytic systems,” *Applied Catalysis*, 375, 172–178 (2010)

Peschel, A., Jorke, A., Sundmacher, K. and Freund, H. “Optimal reaction concept and plant wide optimization of the ethylene oxide process”, *Chemical Engineering Journal*, 207-208, 656-674 (2012)

Rane, V. H., Chaudhari, S. T., and Choudhary, V. R. “Influence of alkali metal doping on surface properties and catalytic activity/selectivity of CaO catalysts in oxidative coupling of methane,” *Journal of Natural Gas Chemistry*, 17, 313–320 (2008)

Rane, V.H., Chaudhari, S. T., and Choudhary, V. R. “Influence of alkali metal doping on surface properties and catalytic activity/selectivity of CaO catalysts in oxidative coupling of methane,” *Journal of Natural Gas Chemistry*, 17, 313–320 (2008)

Rane, V.H., Chaudhari, S.T., Choudhary, V.R. “Oxidative coupling of methane over La-promoted CaO catalysts: Influence of precursors and catalyst preparation method,” *Journal of Natural Gas Chemistry*, 19, 25–30 (2010)

Rufford T.E., Smart S., Watson G.C.Y., Graham B.F., Boxall J., Diniz da Costa J.C., May E.F., "The removal of CO2and N2from natural gas: A review of conventional and emerging process technologies", *Journal of Petroleum Science and Engineering*, 94-95, 123–154 (2012)

Sakakura, T. and Kohno, K. "The synthesis of organic carbonates from carbon dioxide", *Chemical Communications*, 1312 – 1330 (2009)

Salako A.E., Gudmundsson J.S., "REMOVAL OF CARBON DIOXIDE FROM NATURAL GAS FOR LNG PRODUCTION", Semester Project Work, Institute of Petroleum Technology, Norwegian University of Science and Technology, 2005

Salmi T., Roche M., Carucci J.H., Eranen K. and Murzin D., "Ethylene oxide – kinetics and mechanism", *Current Opinion in Chemical Engineering*, 1, 321–327 (2012)

Shafei M., Kabir M.M., Taherzadeh M.J., "Techno-economical study of ethanol and biogas from spruce wood by NMMO-pretreatment and rapid fermentation and digestion", *Bioresource Technology*, 102, 7879–7886 (2011)

Shafei M., Kabir M.M., Zilouei H., Horvath I.S., Karimi K., "Techno-economical study of biogas production improved by steam explosion pretreatment", *Bioresource Technology*, 148, 53–60 (2013)

Shahri, S.M.K., and Pour, A.N. "Ce-promoted $Mn/Na_2WO_4/SiO_2$ catalyst for oxidative coupling of methane at atmospheric pressure," *Journal of Natural Gas Chemistry*, 19, 47–53 (2010)

Shao, Z., Dong, H., Xiong, G., Cong., Y., and Yang, W. "Performance of a mixed-conducting ceramic membrane reactor with high oxygen permeability for methane conversion," *Journal of Membrane Science*, 183, 181–192 (2001)

Shimekit B., Mukhtar H., "Natural Gas Purification Technologies – Major Advances for CO2 Separation and Future Directions", *Advances in Natural Gas Technology*, 235-270 (2012)

Stoukides, M., "Methane Oxidative Coupling: Technical and Economic Evaluation of a Chemical Cogenerative Fuel Cell," *Energy & Fuels*, 9, 794-801 (1996)

Sun J., Ren J., Zhang S., Cheng W., "Water as an efficient medium for the synthesis of cyclic carbonate", *Tetrahedron Letters*, 50, 423–426 (2009)

Sun, J., Thybaut, J.W., and Marin, G.B. "Microkinetics of methane oxidative coupling," *Catalysis Today*, 137, 90–102 (2008)

Tan, X., and Li, K. "Oxidative Coupling of Methane in a Perovskite Hollow-Fiber Membrane Reactor," *Industrial & Engineering Chemistry Research,* 45, 142-149 (2006)

Tan, X., Pang, Z., Gu, Z., and Liu, S. "Catalytic perovskite hollow fibre membrane reactors for methane oxidative coupling," *Journal of Membrane Science,* 302, 109–114 (2007)

Wang, D., Rosynek, M.P., and Lunsford, J.H., "Oxidative Coupling of methane over Oxide-Supported Sodium-Manganese Catalysts," *Journal of catalysis*, 155, 390-402 (1995)

Wang, J., et al., "Comparative study on oxidation of methane to ethane and ethylene over Na2WO4–Mn/SiO2 catalysts prepared by different methods," *Journal of Molecular Catalysis*, 245, 272–277 (2006)

Wang, J.Q., Sun, J., Shi, C.Y., Cheng, W.G., Zhang, X.P. and Zhang, S.J., "Synthesis of dimethyl carbonate from CO2 and ethylene oxide catalyzed by K2CO3-based binary salts in the presence of H2O", *Green Chemistry*, 13, 3213-3217 (2013)

White, J.H., Needham, E.A., Cook R.L., and Sammells, A.F. "The electrochemical oxidative dimerization of methane," *Solid State Ionics,* 53-56, 149-161 (1992)

Wu, J., Qin, S., and Hu, C. "Na_2WO_4/Co–Mn/SiO_2 Catalyst for the Simultaneous Production of Ethylene and Syngas from CH_4," *Catalysis Letters*, 118, 285–289 (2007)

Yoon, K.J., and Seo, S.W. "Oxidative coupling of methane over sodium-salt-promoted zirconia catalysts prepared by the mixed solution method," *Applied Catalysis*, 7, 237-250 (1996)

Zeng, Y., Akin, F.T., and Lin, Y.S. "Oxidative coupling of methane on fluorite-structured samarium–yttrium–bismuth oxide," *Applied Catalysis*, 213, 33–45 (2001)

Zeng, Y., Lin, Y.S., and Swartz, S.L. "Perovskite-type ceramic membrane: synthesis, oxygen permeation and membrane reactor performance for oxidative coupling of methane," *Journal of Membrane Science*, 150, 87-98 (1998)

Zhang, B., et al., "Effective and stable CeO_2-W-Mn/SiO_2 catalyst for methane oxidation to ethylene and ethane," *Natural Gas Conversion VIII*, (2007)

Zheng, W., Cheng, D., Zhu, N., Chen, F., and Zhan, X. "Studies on the structure and catalytic performance of S and P promoted Na-W-Mn-Zr/SiO_2 catalyst for oxidative coupling of methane," *Journal of Natural Gas Chemistry*, 19, 15–20 (2010)

APPENDIX

VITA

Mr. Hattachai Aeowjaroenlap was born in Bangkok, on September 13, 1990. He finished high school from Triamudomsuksanomklao School, Bangkok in 2008. He received his Bachelor's Degree in Chemical Engineering from Chulalongkorn University in 2012. He consecutively continued studying Master degree of Chemical Engineering, Chulalongkorn University since May 2012.